Article:
Li, H. orcid.org/0009-0005-8257-7739, Zhu, Z.-Q. orcid.org/0000-0001-7175-3307, Azar, Z. et al. (2 more authors) (2025) Fault detection of permanent magnet synchronous machines: an overview. Energies, 18 (3). 534. ISSN 1996-1073

https://doi.org/10.3390/en18030534

energies

MDPI

Review

Fault Detection of Permanent Magnet Synchronous Machines: An Overview

Henghui Li [1], Zi-Qiang Zhu [1,*], Ziad Azar [2], Richard Clark [2] and Zhanyuan Wu [2]

[1] School of Electrical and Electronic Engineering, University of Sheffield, Mappin Street, Sheffield S1 3JD, UK; hli214@sheffield.ac.uk
[2] Sheffield Siemens Gamesa Renewable Energy Research Centre, Sheffield S3 7HQ, UK; ziad.azar@siemensgamesa.com (Z.A.); richard.clark@siemensgamesa.com (R.C.); zhan-yuan.wu@siemensgamesa.com (Z.W.)
* Correspondence: z.q.zhu@sheffield.ac.uk

Abstract: These days, as the application of permanent magnet synchronous machines (PMSMs) and drive systems becomes popular, the reliability issue of PMSMs gains more and more attention. To improve the reliability of PMSMs, fault detection is one of the practical techniques that enables the early interference and mitigation of the faults and subsequently reduces the impact of the faults. In this paper, the state-of-the-art fault detection methods of PMSMs are systematically reviewed. Three typical faults, i.e., the inter-turn short-circuit fault, the PM partial demagnetization fault, and the eccentricity fault, are included. The existing methods are firstly classified into signal-, model-, and data-based methods, while the focus of this paper is laid on the signal sources and the signatures utilized in these methods. Based on this perspective, this paper intends to provide a new insight into the inherent commonalities and differences among these detection methods and thus inspire further innovation. Furthermore, comparison is conducted between methods based on different signatures. Finally, some issues in the existing methods are discussed, and future work is highlighted.

Keywords: demagnetization; eccentricity; fault detection; fault signature; inter-turn short-circuit; permanent magnet; permanent magnet synchronous machine

Academic Editor: Marcin Kaminski

Received: 19 December 2024
Revised: 14 January 2025
Accepted: 16 January 2025
Published: 24 January 2025

Citation: Li, H.; Zhu, Z.-Q.; Azar, Z.; Clark, R.; Wu, Z. Fault Detection of Permanent Magnet Synchronous Machines: An Overview. *Energies* **2025**, *18*, 534. https://doi.org/10.3390/en18030534

1. Introduction

Permanent magnet synchronous machines (PMSMs) are becoming increasingly popular in industries due to their high efficiency and high torque density [1]. However, reliability has been one of the major concerns that precludes the further promotion of PMSMs in many safety-critical applications, such as aerospace, electrical vehicles, and wind power generation. To improve the reliability of PMSMs, a lot of effort has been put into this subject from the perspective of the topology and design of PMSMs, the condition monitoring, as well as the fault mitigation and fault-tolerant control. It has been found that condition monitoring could play a vital role in protecting the PMSM drive system from the catastrophic consequences of the faults [2]. In the area of condition monitoring, fault detection is an important subject, which aims at detecting the faults after their occurrence, thus providing information about the type, location, and scale of faults for subsequent emergency operations. On most occasions of online fault detection, the rapidness of detection is also required to reserve enough reaction time.

An extensive body of literature has been published about the fault detection of PMSMs, covering a wide range of faults. In general, the faults in PMSMs could be classified into

three categories based on the failure parts, including electrical faults, mechanical faults, and magnet faults [3], as shown in Figure 1. Electrical faults can be further classified according to the faulty components as winding faults, inverter faults, and sensor faults. Mechanical faults include rotor eccentricity, rotor misalignment, bearing faults, etc. Magnet faults consist of magnet mechanical damage, uniform and partial demagnetization, etc. Winding faults can be further classified according to the failure modes, including inter-turn short-circuit (ITSC) faults, phase-to-phase and phase-to-ground faults, open circuit faults, high-resistance connection (HRC) faults, etc.

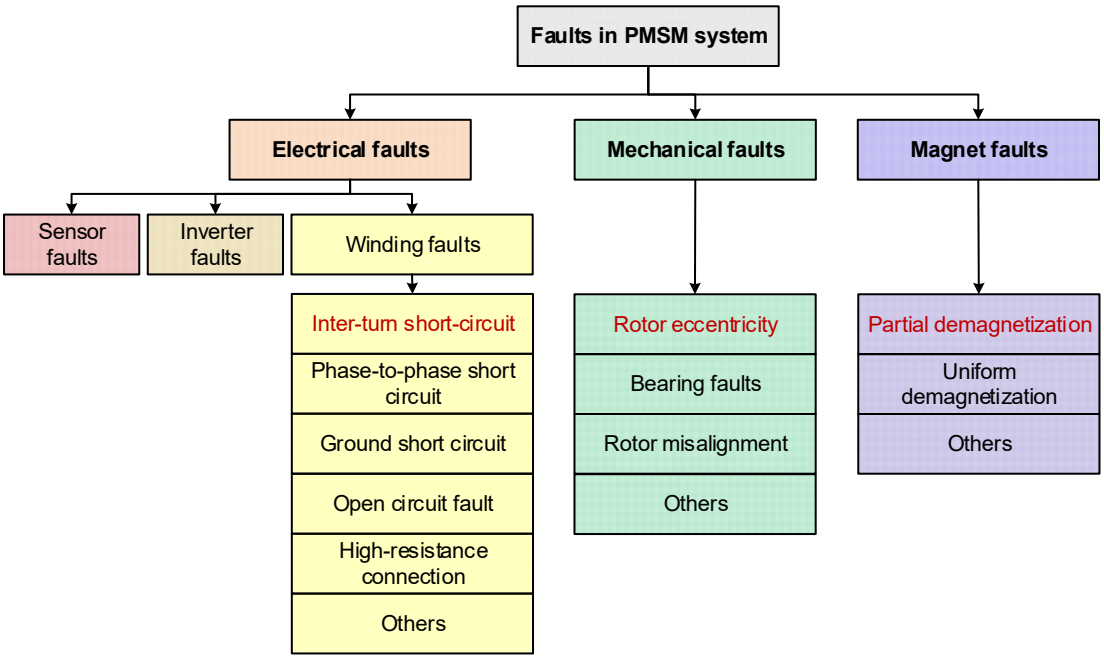

Figure 1. Classification of faults in the PMSM drive system. The detailed explanation of inter-turn short-circuit fault, partial demagnetization fault, and rotor eccentricity fault is shown in Sections 2.1, 3.1 and 4.1.

Several review papers about fault detection have been published. A very comprehensive review is presented in [3] about the fault detection methods. The detection methods are generally classified into three categories: signal-based, model-based, and artificial intelligence (AI)-based methods. Diverse kinds of faults are covered in [3] including ITSC faults, magnet faults, and several kinds of mechanical faults. Special attention is paid to the application of advanced signal processing and AI algorithms; nevertheless, there is a lack of analysis about the signal sources. This could be vital because the available signals might vary dramatically among different applications, and thus, the corresponding fault signatures and the analysis methods might be completely different from each other. In [4], the focus is laid on the detection methods, whereas the corresponding fault signatures are not summarized. Several detailed surveys are accomplished about the detection of ITSC [5], demagnetization [6], and eccentricity [7] faults. However, these papers concentrate more on one fault, thus failing to reveal the common features and differences among these faults, which is critical for distinguishing among these faults. In summary, existing review papers are not systematic and detailed enough. Hence, the target of this paper is to provide a more comprehensive review about fault detection of PMSMs in the perspective of the signals and their signatures.

In this paper, the detection methods of three typical faults in PMSMs are reviewed, i.e., the ITSC fault, PM partial demagnetization (PD) fault, and eccentricity fault, because

they are very common while difficult to detect. The detection methods of each fault are classified into three major categories, i.e., the signal-based, model-based, and data-based methods [3,4,8], as illustrated in Figure 2. Signal-based methods mainly concentrate on extracting the fault-related features of signals directly or indirectly. Model-based methods treat the fault as a variation of the model of the motor, hence using various ways to observe the variation of the model. Data-based methods utilize the algorithms of machine learning, trying to extract high-dimensional hidden information about fault features from the data. Figure 3 concludes the basic principles of signal-, model-, and data-based methods from the perspective of the general fault detection procedure, i.e., feature extraction and decision-making processes.

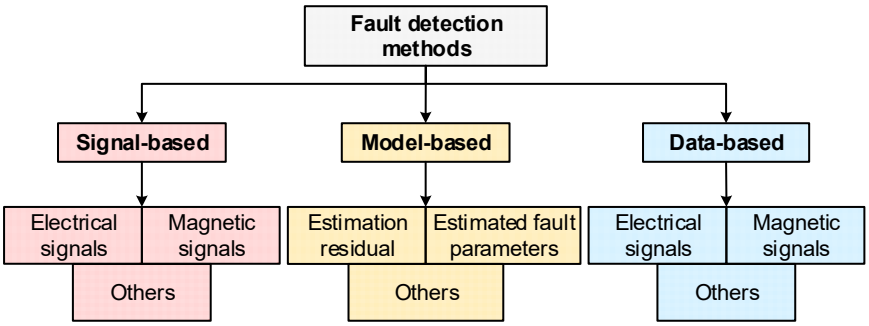

Figure 2. Classification of detection methods for ITSC, PD, and eccentricity faults.

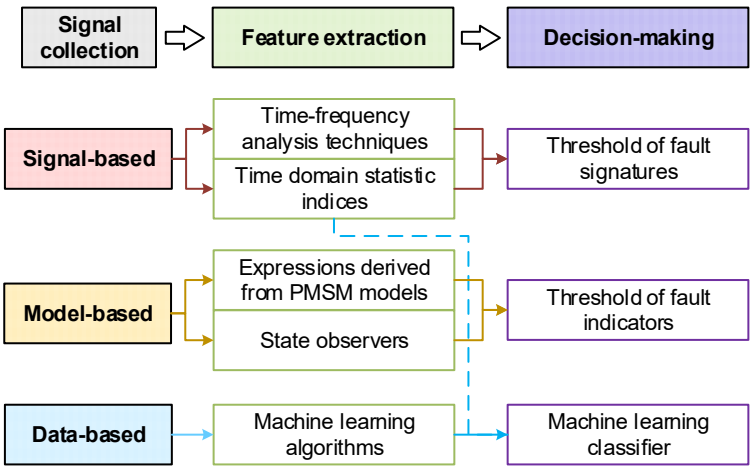

Figure 3. Illustration of fault detection procedure of signal-, model-, and data-based methods.

Furthermore, this paper specifically classifies the papers in the literature according to their signal sources and fault signatures, intending to provide a unique insight into the state-of-the-art techniques for the fault detection of PMSMs and their general issues, as shown in Figure 2.

The contributions of this paper lie in the following aspects:

(1) Classifying and analyzing existing fault detection methods from the perspective of the fault signatures. This paper attempts to dive deeper into the essentials of fault detection methods by focusing on the adopted fault signatures. For example, the model-based methods are divided into methods based on the estimation residual and the estimated fault parameters. In comparison, existing review papers usually make the classification at the level of signal-, model-, and data-based methods. Thus, this paper can provide more detailed guidance for the selection of detection methods in

applications and also provide a clearer landscape about the principles, advantages, and challenges of all these methods.

(2) Mixed collection of newly published papers and classic papers. Fault detection has become one of the hottest topics in recent years, with an increasingly large number of related publications each year. It is important to keep the researchers following the current trends, meanwhile revising the development paths of this area. This paper discusses 46 papers about fault detection published in 2024 and 41 papers published in 2023, while also covering some of the classic papers, such as [9], published in 2006.

This paper is organized as follows. Sections 2–4 discuss the detection methods of the ITSC fault, PD fault, and eccentricity fault, respectively. Section 5 evaluates and compares the reviewed methods. Section 6 discusses some differences in the detection methods of these three faults. Section 7 concludes the paper and presents the future work.

2. Inter-Turn Short-Circuit Fault Detection

2.1. Background

The ITSC fault is the short circuit between one or a few turns of a winding due to the inter-turn insulation degradation and breakdown. The ITSC fault may be the result of various factors including a high winding temperature, mechanical stress, transient overvoltage, etc. When the ITSC fault occurs, the broken insulation part forms a short-circuit path shown in Figure 4a. The residual resistance on the short-circuit path can be modeled as a resistance R_f parallel to the short-circuit part of the winding. The equivalent circuit of PMSMs with the ITSC fault is shown in Figure 4b, where the ITSC fault is assumed in phase A without losing generality.

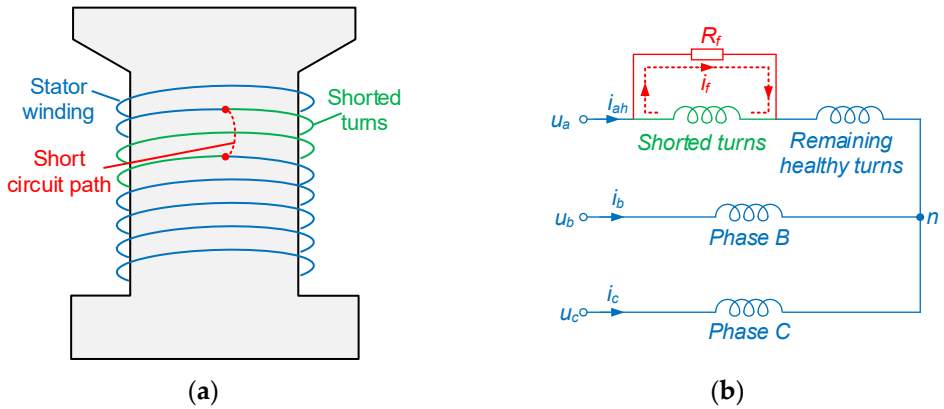

Figure 4. Illustration of ITSC fault. (**a**) Illustration; (**b**) equivalent circuit.

As shown in Figure 4b, a large circulating current i_f will flow through the short-circuit resistance R_f, as well as the shorted coil L_{af}, causing an extremely high temperature in the local area. High temperature can further accelerate insulation degradation, which may lead to the development of an ITSC fault in the manner of an avalanche, resulting in a more serious fault such as a phase-to-phase or phase-to-ground shor circuit [2]. Hence, it is vital to detect the ITSC fault as soon as possible.

However, ITSC fault detection is not easy. The high circulating current does not flow through the regular phase current sensors so that phase currents only contain insignificant fault-related features. Thus, numerous methods are developed to extract and magnify the fault-related features from all types of signals in electrical machines.

2.2. Signal-Based Methods

The signal-based methods refer to those concentrating on extracting explicit signatures from specific signals with time or frequency analysis techniques. The signals adopted for fault detection can be either common electrical signals available in a PMSM drive system or signals obtained with extra sensors such as Hall sensors or search coils. Generally speaking, the signal-based methods can be grouped as electrical signal-based and magnetic signal-based. Obviously, the signatures in electrical signals and magnetic signals are different. Thus, they have different SNR, advantages, and disadvantages. The detailed classification is shown in Figure 5.

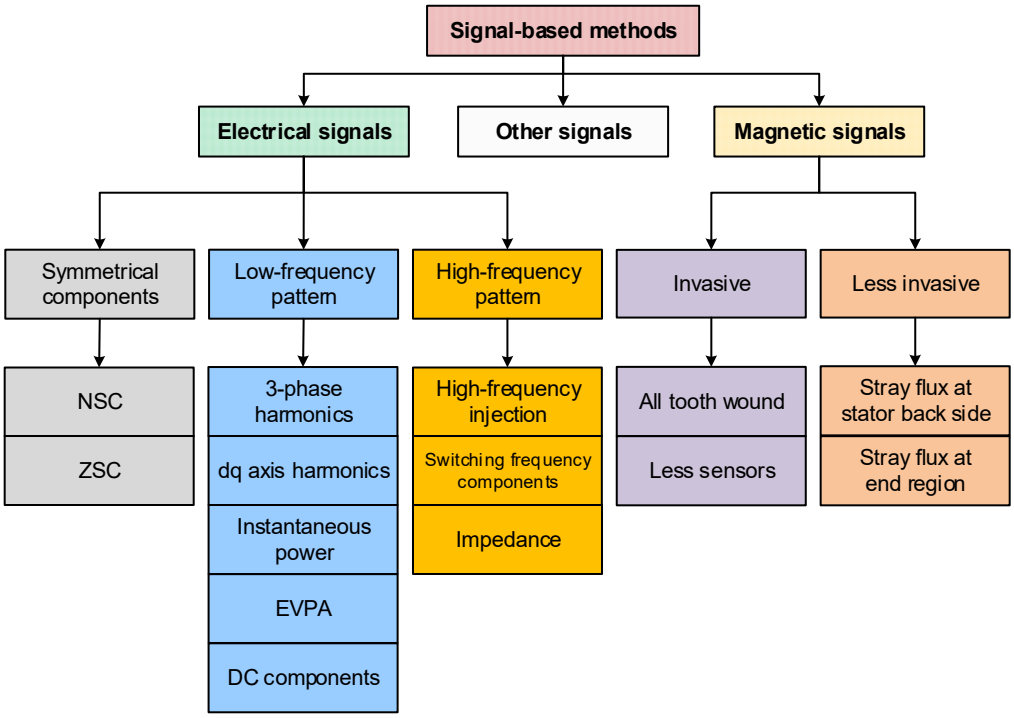

Figure 5. Classification of signal-based methods for ITSC detection.

2.2.1. Electrical Signals

Electrical signals generally include voltage and current signals. Sampled current signals are commonly available in PMSM drive systems due to the need for close-loop control. As for voltage signals, usually the reference voltage signals are used, while extra voltage sensors are usually required to sample the zero-sequence voltage component (ZSVC). In general, the methods based on electrical signals can be grouped according to the type of signatures:

(a) Symmetrical component

Symmetrical component analysis is one of the common ways to detect asymmetry in machines [2,10], where a negative sequence component (NSC) and a zero sequence component (ZSC) emerge in addition to a positive sequence component (PSC). Obviously, an ITSC fault introduces asymmetry in stator winding, and thus, a ZSC and NSC can be found in either machine voltages or currents. A method based on the ZSC in voltage (for wye-connected machines) and current (for delta-connected machines) is proposed in [11]. The location of an ITSC fault can be decided by examining the phase angle information of a ZSC, which is also found able to discriminate between HRC and ITSC faults [12]. These methods are further integrated with mitigation methods in [13,14]. The similar idea is applied in brushless DC (BLDC) machines with a simple fault severity evaluation method [15], reducing the impact of working conditions on fault detection. Laadjal et al. [16]

propose a fault index defined as the ratio between ZSC, NSC, and PSC so that the ITSC fault can be distinguished from unbalanced supply voltage. The algorithm is improved by introducing short-time least-squares Prony's algorithm to track the fundamental frequency component [17,18]. In [19], the ZSC in voltage is found to have a better signal-to-noise ratio (SNR) and sensitivity to faults than the second harmonics in q-axis current and the speed harmonics.

Similar to ZSC, NSC will emerge in the voltage or current of machines [20]. Jeong et al. [21] successfully utilize the NSC in machine voltages to detect the ITSC fault of PMSMs. It has also been found that NSC in voltage is more sensitive to ITSC faults and is more general compared to ZSC in voltage because the amplitude of ZSC in voltage is dependent on the leakage inductance of the machine. Meanwhile, NSC in current can also be utilized to detect ITSC faults [22]. A fault indicator is further proposed in [23] by combining the NSC and PSC in current. The phase angle between NSC and PSC in current is used to locate the ITSC fault. Furthermore, NSC in voltage and current can be utilized at the same time. A novel fault indicator is proposed in [24], which is the phase shift between NSC in the machine voltage and current. The indicator can discriminate the unbalanced load of the PM synchronous generator (PMSG) and the ITSC fault; meanwhile, the location of the ITSC fault is revealed by the phase angle of the NSC in voltage. Similarly, the NSC in voltage can also be combined with ZSC and PSC to detect ITSC faults [16,25].

(b) Low frequency (LF) pattern

On the other hand, the frequency pattern of signals usually also contains effective signatures for ITSC detection. From the perspective of the way to obtain frequency patterns, diverse frequency analysis techniques are adopted in the existing literature, such as fast Fourier transform (FFT) [26–29], orthogonal phase-lock-loop (PLL) [30,31], empirical model decomposition (EMD) [32,33], wavelet transform [34], etc.

Meanwhile, existing methods also cover a wide range of fault signatures. For example, third harmonics in phase currents are found feasible for detection [32], thus being tracked with quadratic time–frequency techniques, targeting fault detection in non-stationary situations. Dogan et al. [33] extract third harmonics in phase currents using Gabor transform and ensemble EMD. Lee et al. [28] made a conclusion that the negative frequency part of third harmonics is free from supply imbalance and inherent structural asymmetry, leading to its high robustness. The ITSC fault signatures are selected as $(2k-1)$th harmonics in [27], which is a more general fault signature. Naderi et al. [26] obtain the fault-related frequency signatures in the currents of PMSM through comprehensive theoretical analysis, concluding the capability of each frequency component to distinguish among different faults.

The frequency pattern in dq-axis quantities is also widely applied. It is discovered that ITSC fault introduces second harmonics in dq-axis voltage and currents [35], which can be treated as an alternate perspective of the same fault signatures with NSC [2]. However, the variation in controller bandwidth will cause re-distribution of the second harmonics between voltage and current [36]. Huang et al. [31] introduce a fault index called the Rayleigh quotient so that the second harmonics in voltages and currents can be spontaneously synthesized to reduce the influence of current controller bandwidth. The second harmonics extraction method can be improved by applying a short-time Adaline neural network [37], variational mode decomposition (VMD) [38], and wavelet transform [39]. The transient false alarm is mitigated in [40] through estimated compensation signals calculated according to the mechanical closed-loop transfer function. There are also methods using the second harmonics in the extended Park's vector approach (EPVA) [41].

Power, which is essentially the multiple of voltage quantities and current quantities, combines both the signatures from voltage and current. The second harmonic is found to appear in instantaneous reactive power (IRP) when an ITSC fault occurs in a PMSM

working in the motoring mode, while it appears in instantaneous active power (IAP) in the generating mode [29]. The analysis results show the amplitude of the second harmonics in IRP or IAP is sensitive to working conditions. Consequently, the look-up table (LUT) is adopted to make a fault decision. A similar detection method is proposed in [42], where the second harmonics are observed in the instantaneous power of a synchronous generator.

Information in the amplitude and phase angle of the fundamental frequency component in phase voltages or currents, i.e., the DC components in dq-axis quantities, are utilized in some papers for ITSC fault detection and discrimination from other faults. The voltage vector variation in the dq-axis is used as the fault indicator in [43]. The static eccentricity fault, PM and PD faults, and ITSC fault cause the voltage vector to deviate from a healthy vector toward a different direction. Meanwhile the deviation of the current angle is found to increase when an ITSC fault occurs while demagnetization causes the current angle to decrease [44]. Similarly, the torque angle is utilized in [45], which is essentially the angle between the voltage vector and the d-axis. The amplitude and phase differences among $\alpha\beta$ fundamental frequency currents are considered together in [46]. It is worth mentioning that, recently, the fundamental frequency components in the xy subspace of dual three-phase PMSM (DTPPMSM) were found to be feasible for detecting and locating an ITSC fault [30,47–49].

(c) High-frequency (HF) pattern

Previously mentioned papers mainly concentrate on frequency patterns in the LF range. As for patterns in the HF range, two types of methods are developed, i.e., methods based on the switching of frequency components and those based on the HF injection.

Switching frequency components exist in a switching inverter-based drive system. It is a naturally embedded excitation source providing useful information for fault detection. Sen et al. [50] observe that the admittance of phase winding increases in the HF region after an ITSC fault happens. Hence, switching frequency ripple is adopted as the HF test signal to obtain the HF impedance of winding. A similar idea is also investigated in [51]. Hu et al. [52] model and analyze the pulse-width modulation (PWM) signals in a PMSM and obtain the analytical expression of the PWM ripple current. The analytical expression, as well as the simulation, shows that the amplitude of the PWM ripple current of the faulty phase increases when the ITSC fault occurs. A fault index is further proposed, defined as the ratio of the $2f_{switching}$ component in adjacent phases. The same principle is adopted in [53], while its capability to distinguish between a high-resistance connection (HRC) and an ITSC fault is discovered. An HRC fault only causes resistance asymmetry, hence it is insensitive to HF voltage, while ITSC causes inductance variation, hence the discrimination of two kinds of faults. The method is improved by the combination of the ZSVC and switching frequency component analysis [54]. The fundamental component of ZSVC is used to detect asymmetry in the stator while the HF component in ZSVC is used to distinguish between the HRC and ITSC faults. Meanwhile, Gao et al. [55] combined the NSVC and switching frequency component analysis. Wang et al. [56] compare interior PMSMs (IPMSMs) and surface-mounted PMSMs (SPMSMs), where the saliency ratio is proved to be insignificant to the switching frequency and its sideband in the current spectrum.

Switching frequency components in voltage rely on the modulation index, thus being influenced by working conditions. On the other hand, by injecting HF voltage or current, the excitation source becomes independent from working conditions, making fault signatures much more consistent across different working conditions. A method based on the HF rotating current is proposed to distinguish between HRC and ITSC faults [57]. The injected frequency component is extracted from ZSVC. Xu et al. [58] inject specially designed HF currents so that the injected currents only flow through two phases at one time. The line voltage difference when injecting different pairs of phases is selected as the fault indicator.

Other than the current injection, rotating square wave voltage is injected in [59,60] and the differences of the HF response in three phases are selected as the fault features. Different kinds of signal injection methods, including rotational voltage, static pulsating voltage, rotational pulsating voltage, and rotational current, are systematically compared in [61]. The rotational voltage injection with constant amplitude is found to have more significant fault features while having a simpler injection structure than the others. The HF injection method is improved in [62] by replacing the zero voltage vector in the output of space vector PWM (SVPWM), which results in a spatially asymmetrically distributed rotating HF voltage. The capability of locating ITSC and HRC faults with a high-frequency injection is further extended in [63].

Impedance can be calculated based on signal injection. It can be seen as another perspective to evaluate the ITSC fault. Qi et al. [64] find that ITSC faults and eccentricity have different influences on the impedance over the whole region of magnetic working points, which can be used to distinguish these two faults. Another different way of utilizing impedance information is presented in [65], where the resistance of phase winding is used as the fault indicator. When ITSC fault occurs, the resistance of the corresponding phase reduces, leading to a reduction in d-axis resistance, which is estimated by injecting DC voltage under the standstill condition.

(d) Others

Apart from the aforementioned methods, there are various ways of extracting fault signatures from current and voltage. Hang et al. [66] provide a novel method that uses the differences among the three-phase current amplitudes as the fault indicator. Obeid et al. [67] manage to detect the distortion in phase current or voltage waveforms caused by intermittent ITSC faults using adaptive wavelet transform. The cost function of the model predictive control system is utilized as a fault signal source in [68]. Discrete wavelet transform (DWT) is adopted to analyze the cost function signal since it is a non-stationary signal. ITSC fault is detected by monitoring the normalized energy-related feature vector calculated from the wavelet transform coefficients. Skewness of currents [69], current envelope [70], and the model signal of phase currents [71] are also found to be effective for the detection of ITSC faults.

2.2.2. Magnetic Signals

Unlike electrical signal-based methods, magnetic signal-based fault detection methods extract fault signatures through the magnetic field. These methods provide a different view of the ITSC fault. As shown in Figure 6, different mounting places of sensors require different levels of modification to the machine. According to the significance of the modification, magnetic signal-based methods can be classified into two kinds, i.e., invasive methods and less-invasive methods. Since the flux distribution varies in space, the signals captured in different places are certainly different, and thus, different fault features are discovered with these two kinds of methods.

(a) Invasive methods

Invasive methods place the sensors on the main flux path of the machine, as shown in Figure 6a. Thus, sensors are usually placed in the slots [72,73], stator yoke [74], around the tooth coils [75], etc., meaning that significant modification of the machine is required. Da et al. [72] utilized the search coils on all teeth for the detection of various faults. The polar diagram is then drawn to see the distortion of the airgap flux linkage due to an ITSC fault. Similarly, Zeng et al. [76] also use search coils wound on a tooth. The frequency components $(2h_k \pm 1)f_e$ (h_k is the carrier wave ratio) are found to have high SNR, and a fault index based on these two components is proposed.

On the other hand, only six search coils are required in [73] by setting the coil pitch of the search coils the same as the coil pitch of the phase windings. The NSC, with a frequency of $2f_s \pm f_e$, component is extracted as the fault indicator, where f_s is the switching frequency. Furthermore, a universal design method for search coil structure is developed in [77], considering the reliability, sensitivity, SNR, and positioning capability of the induced voltage.

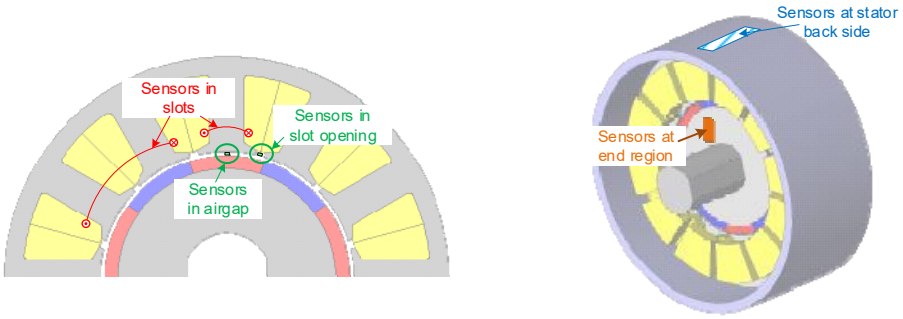

(**a**) (**b**)

Figure 6. Illustration of typical mounting placing of flux sensors for fault detection. (**a**) Invasive methods; (**b**) less-invasive methods.

(b) Less invasive methods

Compared with the invasive methods, less-invasive methods make less significant modifications to the machine. The sensors are usually placed at the end region or outer side of the stator back iron, as shown in Figure 6b. Liu et al. [78] build and analyze the magnetic equivalent circuit model of a PMSM and find that the stray flux at the stator back side changes with the magnetomotive force (MMF) of the windings. Thus, tunneling magneto-resistive (TMR) sensors are placed at the stator back side to obtain the stray flux density. A polar diagram is drawn to discover the distortion in spatial distribution. A similar method using only two search coils at symmetrical positions of the stator back side is proposed in [79]. The Pearson correlation coefficient is adopted to analyze the induced voltage in two search coils. Gurusamy et al. [80] specifically use the third harmonics in stray flux to detect ITSC faults in PMSMs because the fundamental frequency component may lead to a false negative error. Eldeeb et al. [81] propose a different method by utilizing the switching frequency components in the stray flux, where an antenna placed relatively far away from the machine is used to extract the switching frequency and its odd number multiple components.

The housing of the machine may affect the stray flux distribution at the stator back side. In such cases, placing sensors at the end region is an alternative way. Assaf et al. [82] analyze the spectrum of the axial stray flux as well as the sensitivity of different frequency components to ITSC faults and unbalanced supply. Lamim et al. [83] place two stray flux sensors at the end region, which are orthogonal to each other. An orbit diagram is used to illustrate the distortion of the leakage flux linkage. Kumar et al. [84] combine temperature and the leakage flux density together for ITSC faults.

2.2.3. Other Signals

Other signals are also utilized for ITSC fault detection, such as mechanical signals [85] and temperature signals [84,86]. For example, since the ITSC fault leads to harmonics in currents, it can be expected that these will excite corresponding mechanical responses. Hence, the fourth harmonics in speed signals [38,87,88] and vibration signals [85] are investigated for ITSC fault detection.

2.2.4. Summary

Table 1 concludes the general advantages and disadvantages of different kinds of signal methods discussed in this section. Table 2 summarizes some of the typical research, its contributions, and aspects for further improvements.

Table 1. Comparison among signal-based methods of ITSC detection.

Signal Types	Fault Indicator Types		Advantages	Disadvantages
Electrical signals	Symmetrical components	ZSC	+ Suitable for online detection + Irrelevant to winding topology and pole-slot combination	- Troublesome to measure ZSC voltage
		NSC	+ Irrelevant to winding topology and pole-slot combination + Higher amplitude than ZSC + Easier to obtain	- Affected by unbalanced input
	LF pattern	Three-phase harmonics	+ Easy to obtain + Readily integrated in the control system	- Difficult for transient process - Usually high computational burden
		dq-axis harmonics		- Influenced by winding topology
		Impedance	+ Less influenced by controller bandwidth	- Influenced by saturation/temperature
		Instantaneous power	+ Less influenced by controller bandwidth	- Sensitive to load and speed - Low sensitivity at no-load condition
		Others	+ Easy to obtain	- Not suitable for transient process
	HF pattern	Injection	+ Steady sensitivity + Suitable for a wide range of loads and speeds	- Vibration and noise - Influence on control performance
		PWM related	+ High SNR	- Low sensitivity at no-load condition - Difficult to sample PWM ripple current
Magnetic signals	Invasive		+ High SNR	- Invasive - Usually need many sensors
	Less invasive	Stator back side	+ Less invasive	- Influenced by housing
		End region		- Low SNR

Table 2. Typical research among signal-based methods for ITSC detection.

		Typical Works	Solved Problems	Unsolved Problems	Primarily Challenges
Electrical signals	Symmetrical components	[11]	Detection and localization of fault using ZSC signal	Model is only applicable for SPMSM	Monitoring faults in non-stationary conditions
	LF pattern	[40]	Mitigation of transient process impact	Compensation is dependent on machine parameters	Saturation can affect performance of compensation
	HF pattern	[52]	Consistent fault indicator irrelevant to modulation index	The required sampling frequency is very high	Reduction in the cost of extra sampling board
Magnetic signals	Invasive	[72]	Distinguish between different kinds of faults	Large amount of search coils	Reduction in number of search coils
	Less invasive	[78]	Analytical analysis of stray flux	Large amount of TMR sensors	Reduction in number of sensors

2.3. Model-Based Methods

Instead of explicitly extracting certain time or frequency domain features from signals, model-based methods utilize the mathematical or finite element method (FEM) models of PMSMs to estimate fault-related quantities. Compared with signal-based methods, model-based methods rely more on the machine parameters but are usually more suitable for transient conditions.

To better reveal the essential differences between these methods, in this paper model-based methods are classified according to their observed signatures. For ITSC fault detection, the commonly used signatures include the estimation residual, estimated shorted turn ratio, etc., as shown in Figure 7.

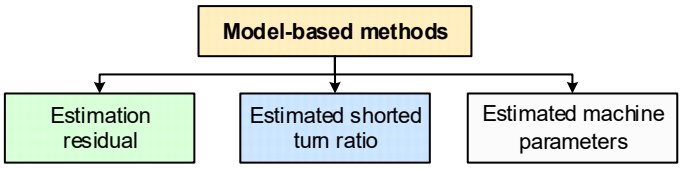

Figure 7. Classification of model-based methods for ITSC detection.

2.3.1. Estimation Residual

Healthy PMSM models are commonly used in this category of detection methods. When the ITSC fault occurs, the model of the real machine becomes different from the assumed healthy model, causing errors in the estimation results. Hence, the estimation errors can be used as a fault indicator.

Three-phase current residuals are estimated with open-loop calculation in [89]. Meanwhile, an $\alpha\beta$ current observer with feedback is adopted in [90] to calculate current residuals considering the non-linearity of the inverter model and unbalanced inductance. Mazzoletti et al. [91] further consider the influence of parameter errors. It is proved that NSC in the current estimation residual is independent of parameter errors, hence being used as a fault indicator to reduce the influence of the parameter variation. The NSC of the residual is also selected as the fault indicator in [92], but the current estimation is achieved with the assistance of FEM so that the saturation effect can be considered. The FEM model provides the relationship between dq-axis flux linkages and currents. A similar principle is adopted in [93] while the influence of working conditions is mitigated with a LUT. Mahmoudi et al. [94] use the Luenberger observer to estimate the dq-axis currents. The NSC in the estimation residual is still used as the fault indicator. A full-order Luenberger observer [95] and the extended Kalman filter [96] have also been investigated for residual calculation. To better account for parameter uncertainty and nonlinearity, digital twin models are used to obtain the current residuals [97].

Similar to current residuals, voltage residuals are also utilized. Hang et al. [98] model the PMSM under the ITSC fault condition with two terms of voltage disturbances at the dq-axis, and use the Luenberger observer to estimate the voltage disturbances. The sum of two voltage disturbances is taken as the fault characteristics signal, and the 2nd harmonics in it is used as the fault indicator. Similarly, Du et al. [99] estimate the disturbance in back-EMF with an extended state observer and extract the 2nd PSC in the disturbance as the fault indicator. A five-phase PMSM is investigated in [100], where the voltage disturbances in all phases are estimated.

Other than currents and voltages, various physical quantities can also be estimated to monitor the deviation of the machine model due to the occurrence of a fault. Sarikhani et al. [SAR13] estimate the back-EMF of PMSM and, similarly, take the residual of estimation as the fault indicator. However, the fault index is set to the linear average of residual normalized against speed. Cui et al. [101] estimate the electromagnetic torque using the torque equation under the healthy condition. The estimation error is obtained by subtracting the estimation value from the real value measured with the torque transducer. Through theoretical analysis,

the DC component in the residual is found to only exist when the ITSC fault occurs, thus being used as the fault indicator. Xu et al. [102] analyze the model of a sensorless SPMSM with an ITSC fault considering the inverter nonlinearity and the current measurement error. The residual voltages in the estimated *dq*-axis contain various harmonics when an ITSC fault happens. With a proper harmonics elimination algorithm, the eighth harmonics in the voltage estimation residual are selected for ITSC fault detection.

Upadhyay et al. [103] estimate the flux linkage in the *dq*-axis and draw the XY diagram to observe the trace of flux linkage. By extracting the DC component in the flux linkage trace variation, the fault can be detected and located.

For DTPPMSM, Yang et al. [104] utilize the difference of voltage vectors of two sets of windings to detect the ITSC fault.

Furthermore, the model-based method can be combined with the high-frequency injection method for better SNR by estimating the high-frequency injection residual [105,106].

2.3.2. Estimated Shorted Turn Ratio

This kind of method utilizes the PMSM model with ITSC fault. The faulty model contains the shorted turn ratio as a parameter. Thus, the short-circuit ratio can be estimated with the information in machine voltages or currents, either through open-loop expressions [107], or closed-loop observers [108,109].

Aubert et al. [108] build a PMSM model consisting of the standard PMSM voltage equations and the short-circuit loop voltage equation. The Kalman filter is adopted to estimate the shorted-turn ratio of each phase. Sayed et al. [109] take a similar approach, but also compare the performance of the extended Kalman filter and the unscented Kalman filter. Furthermore, a hidden Markov model is adopted in [110] to estimate the range of the shorted turn ratio and short-circuit resistance.

2.3.3. Estimated Machine Parameters

ITSC faults lead to changes in machine parameters such as inductances and back-EMFs. Hence, detection of ITSC faults can be achieved with parameter estimation methods [8,111,112]. In comparison of methods based on estimation residuals, these kinds of methods estimate the parametric quantities instead of machine variances, meaning that the estimated parameters should be time-invariant under constant working conditions. In [113], the inductances, the turn numbers of the phase windings, and the phase resistances are estimated to detect ITSC faults. In [114], the probability distribution function of estimated machine parameters is used as the fault indicator.

Except for the aforementioned methods, several other fault indicators have also been investigated, such as estimated torque [115], speed estimation residual [116], etc.

2.3.4. Summary

Table 3 concludes the general advantages and disadvantages of different kinds of model-based methods discussed in this section. Table 4 summarizes some of the typical research, its contributions, and aspects for further improvements.

Table 3. Comparison among model-based methods of ITSC detection.

Signatures	Advantages		Disadvantages	
Estimation residual	+ Less computational burden	+ Suitable for non-stationary conditions	- More estimated variables	- Dependent on machine parameters
Estimated shorted turn ratio	+ Easy to evaluate fault severity			
Estimated machine parameters				

Table 4. Typical works among model-based methods for ITSC detection.

	Typical Works	Solved Problems	Unsolved Problems	Primarily Challenges
Estimation residual	[92]	Reduction in the influence of saturation effect	LUT is required for different working conditions	Large memory consumption of storing LUT
Estimated shorted turn ratio	[108]	Direct estimation of SC ratio in each phase	Assuming the SC resistance is about 0 Ω	Feasibility when SC resistance is not near 0 Ω
Estimated machine parameters	[114]	Combining parameter estimation with probabilistic fault detection	Cannot tolerate a large difference between L_d and L_q.	Accounting for large saliency machine

2.4. Data-Based Methods

Compared with signal- and model-based methods, data-based methods generally use a significantly larger amount of machine operating data. Fault signatures in the data are extracted and analyzed implicitly through the machine learning process, while the machine model and explicit fault signatures are usually less important.

Data-based methods can be classified according to the signals they used: electrical signals, magnetic signals, and other signals, as shown in Figure 8.

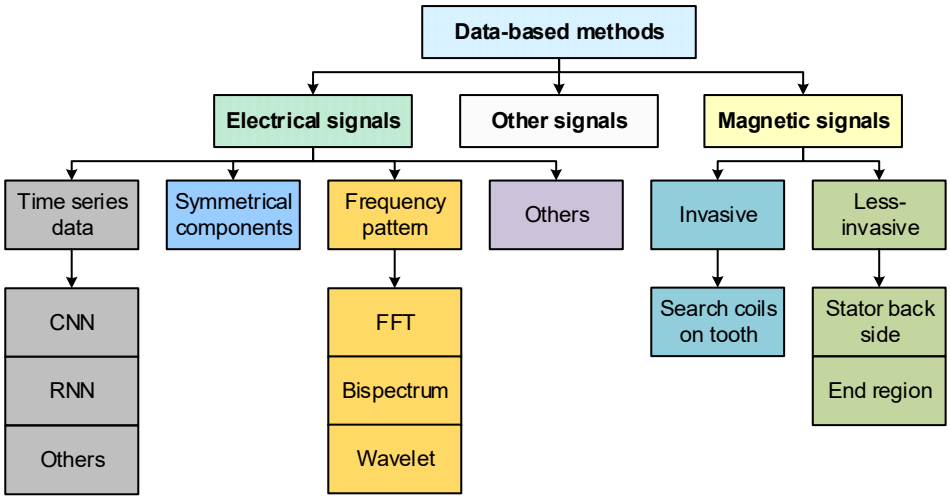

Figure 8. Classification of data-based methods for ITSC detection.

2.4.1. Electrical Signals

Machine learning algorithms put no limit on the input data forms. Some algorithms, such as CNN or recurrent neural networks (RNNs), can directly process the time series data, and the implicit fault features are automatically learnt from the training data. In contrast, fault signatures in the time series data can also be processed with signal analysis tools such as FFT, and the fault-related information in the results can be subsequently extracted with machine learning algorithms. Thus, the methods are further classified according to the forms of input data of machine learning algorithms.

(a) Time series data

Data in the form of time sequence can be directly fed into the machine learning algorithms. Thus, the fault signatures are automatically determined and extracted with machine learning processes and then are analyzed and classified. In [117], three-phase voltage and current signals are directly input into the proposed framework. Multiple feature extraction methods, as well as multiple classifications, are used in parallel and synergized with Fisher's ratio. Wang et al. [118] manage to detect an ITSC fault with two

of the three phase currents and the deep autoencoder. Furthermore, only one phase current is required in [119].

A wide range of existing methods apply the convolutional neural network (CNN) for fault detection. The convolution layer usually plays a role as the feature extraction method in the machine learning structure. Compared with traditional spectrum analysis tools, such as FFT, the corresponding features are identified and extracted with the convolution layer self-adaptively according to the training data, because the convolution core is obtained through a training process. In [120], a method based on CNN is proposed, where time series of three-phase currents compose a $3 \times n$ array as the input of CNN. Shih et al. [121] compare the performance of SVM and CNN on ITSC fault detection. Time series of q-axis voltage and current are used as the input of SVM, while the waveforms of them are converted into 2D images and fed into CNN. A conclusion is made that SVM, which is assisted with a mathematical model of PMSM, requires much less data. On Bayesian optimization-based residuals, CNN is applied in [122] to reduce network depth and avoid the degradation effect when feeding time series data into CNN. A residual dilated CNN is applied in [123], combined with transfer learning techniques. Some other applied methods, such as deep Q-network [124] and stacked autoencoder [125], also have one or multiple convolutional layers.

Apart from CNNs, transformer neural networks [126], RNNs [127], etc., can also learn the features from time series data.

Furthermore, it is worth noting that traditional artificial intelligence algorithms are also widely applied to select certain features for fault detection [128] or estimate fault-related quantities [129], such as genetic algorithms (GAs) [113,130,131], particle swarm optimization (PSO) algorithms [128,129], and fuzzy logic algorithms [132–134]. In [113], a GA is adopted to estimate the inductance parameters whose variation contains fault-related information. Similarly, PSO is adopted in [129]. In [131], a PSO algorithm, GA, and a whale optimization algorithm, as well as the stochastic parallel gradient descent algorithm, are successfully applied to detect ITSC faults under different non-ideal conditions. It was also found that the stochastic parallel gradient descent algorithm is more stable than the others. The fuzzy logic algorithm is adopted in [132] to straightforwardly map the nonlinear relationship between machine currents and speed to the state of the machine. This method is improved by combining ANN with fuzzy logic in [135], called an adaptive neural fuzzy inference system.

(b) Symmetrical components

Instead of directly feeding three-phase current signals, NSC and PSC are used as the input for a neural network in [136]. Similarly, an attention-based RNN is adopted in [127] to analyze the NSC, PSC, and speed. Meanwhile, Pietrzak et al. [137] take NSC and PSC as the input of the k-nearest neighbor (KNN) algorithm.

In [138], an efficient method based on stacked sparse autoencoders and Siamese networks is proposed to reduce the amount of data required for training. Seven kinds of signals and features are integrated into the dataset, including a three-phase current, NSC and PSC in current, NSC impedance, and electronic torque.

(c) Frequency pattern

Machine learning algorithms can also process the spectrum of three-phase currents [139,140] or dq currents [141]. Specifically, Pietrzak et al. [142] use bispectrum analysis to pre-process three-phase currents. The result of the bispectrum analysis is a 2D image, which is then fed into a CNN for further feature extraction. Meanwhile, other time-frequency analysis techniques, such as the wavelet transform [143], are also adopted.

(d) Other features

The image of Park's vector trajectory is used as the input of a neural network in [144]. In [145], 15 features are extracted from current signals to build up the dataset, including mean value, maximum value, root-mean-square (RMS) value, etc. In [146], the differences between two of three phase currents are obtained to enhance the fault signatures.

The estimation residual of a q-axis current based on a Luenberger observer is used in [147] so that the information of the PMSM model can be incorporated into the machine learning process.

It is worth noting that the hybrid methods of signal-based methods and data-based methods become more and more popular due to their special advantages. The signatures extracted with signal-based methods, such as harmonics and sequence components, are fed into AI algorithms so that the hidden information in the multiple signatures can be learned and used for the improvement of detectability. Compared with solely signal-based methods or data-based methods, the hybrid methods [136–138] rely less on the process of learning the implicit features and also show an improvement in detection accuracy.

2.4.2. Magnetic Signals

Search coils are placed on a tooth to capture the abnormality in airgap flux density distribution due to the ITSC, eccentricity, and partial demagnetization fault in [148], where the induced voltage is processed into an image using a short-time Fourier transform. Meanwhile, the stray flux density in the end region [149] and at the stator back side [150] are also investigated.

2.4.3. Other Signals

Apart from the electrical and magnetic signals, many other signals are also used for ITSC detection. For example, torque signal is combined with currents in [124]. Speed signal is combined with dq voltage and currents in [141] to reduce the influence of controller bandwidth. Furthermore, the input current on the power side [151] and the vibration signals [152] are also investigated.

2.4.4. Summary

Table 5 concludes the general advantages and disadvantages of different kinds of model-based methods discussed in this section. Table 6 summarizes some of the typical research, its contributions, and aspects for further improvements.

Table 5. Comparison among data-based methods of ITSC detection.

Input Data Types			Advantages		Disadvantages
Electrical signals	Time series	+	Non-invasive	-	Difficult to integrate the information about widely adopted fault harmonics
		+	No need for choosing signal analysis tools		
	Symmetric components	+	Non-invasive	-	May be limited by the information in the extracted features
	Spectrum	+	High sensitivity		
Magnetic signals	Airgap flux density	+	High sensitivity	-	Invasive
	Stray flux density			-	Relatively low SNR

Table 6. Typical works among data-based methods for ITSC detection.

Typical Works	Solved Problems	Unsolved Problems	Primarily Challenges
[147]	Integrating known information about faulty models into AI	Influenced by parameter errors	Enhance the robustness against parameter mismatch and immunity against transient process
[122]	Simplify hyperparameter tuning process	Influenced by working conditions	Robustness against variation of working conditions

3. Partial Demagnetization Detection

3.1. Background

Demagnetization of a magnet means the magnetic property of this magnet degrades. Once the applied field strength exceeds the knee point of the B-H curve of a PM, as shown in Figure 9, the working point of the PM will not recover following the original B-H curve but will follow the recoil line [153]. This means that the remanence is reduced from B_r to $B_r^{'}$; in other words, the PM is demagnetized. Generally, a high temperature and large armature field are the main causes of demagnetization faults [154]. The demagnetization severity of a PM is usually reflected in its remanence B_r, which decreases as the severity of demagnetization increases.

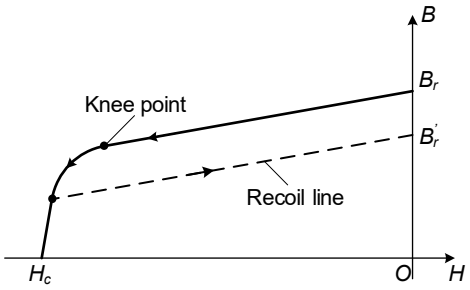

Figure 9. Illustration of demagnetization curve of a PM.

In the area of fault detection, PM demagnetization faults are usually classified into two categories: uniform demagnetization (UD) and PD. UD means all PMs in a PMSM are demagnetized uniformly, while PD means only one or a few PMs are demagnetized, and the severity of demagnetization can be non-uniform. In recent research, PD detection gains more attention due to its commonness and difficulties in detection. Hence, this paper concentrates most on PD detection rather than UD detection.

PD causes unwanted harmonics in the back-EMF and currents, as well as torque ripple, unbalanced magnetic pull, and vibration [3], leading to a deterioration in the performance and efficiency of the PMSM drive system.

Detection of PD has been widely investigated in the past few decades. The proposed methods can be classified into signal-based, model-based, and data-based, similar to the ITSC detection methods.

3.2. Signal-Based Methods

Classification of signal-based methods for PD detection is shown in Figure 10.

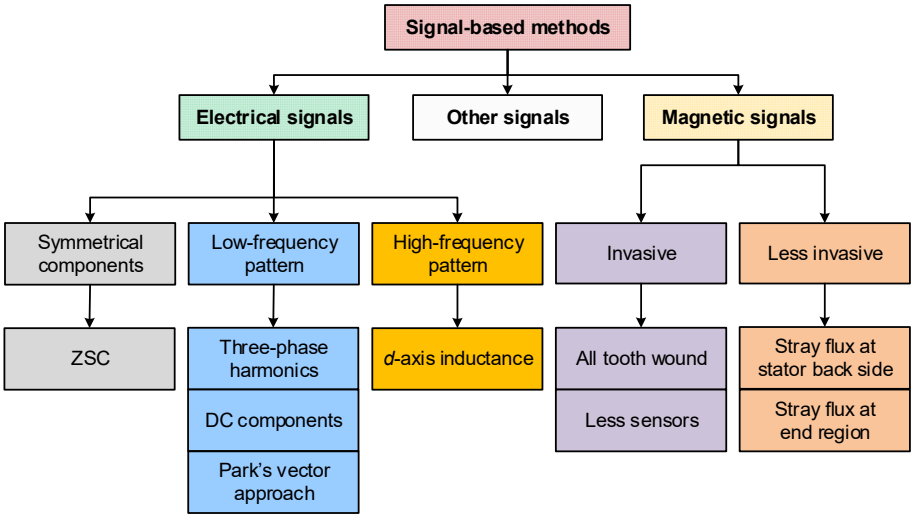

Figure 10. Classification of signal-based methods for PD detection.

3.2.1. Electrical Signals

(a) Symmetrical components

Similar to ITSC fault detection, symmetrical component analysis can also be applied in PD detection. The mostly used symmetrical component in PD detection is ZSC. Urresty et al. [155] discuss the influence of winding configurations on the spectra of currents and ZSVC of a PMSM with a demagnetization fault. It is proved that harmonics appear in both the current spectrum and ZSVC spectrum in fractional-slot PMSM in the case of PD. But in integral-slot PMSM, new harmonics may not emerge in the current or ZSVC spectrum, depending on the specific winding configuration. It is also discovered in [156] that fractional harmonics in the current spectrum related to PD might be cancelled in the phase current with certain winding configurations. However, the ZSVC will not be eliminated in such a winding configuration, hence it being eligible for PD detection. Furthermore, Zhan et al. [157] extend the ZSC-based methods to DTPPMSM. The drop of the third harmonics in the difference of ZSVC in two sets of windings is chosen as the fault indicator for an integer-slot machine, while, for other types of machines, the fractional harmonics are used.

(b) LF pattern

Fractional harmonics are very frequently used in demagnetization fault detection. When PD occurs, the frequencies of harmonics that emerge in three-phase currents can be expressed as [158]

$$f_{PD} = f_e\left(1 \pm \frac{k}{p}\right), k = 1, 2, 3, \cdots, \quad (1)$$

where f_e is the electrical frequency, p is the pole-pair number, and k is any positive integer.

According to the pole number of a certain machine, the corresponding fault harmonics can be obtained FFT [159]. However, under the transient condition, the fundamental frequency components interact with fault-related harmonics [160], causing a false alarm. Thus, advanced signal processing techniques are adopted to track and analyze the harmonics, such as wavelet transform [161], the box-counting algorithm [162], the Vold–Kalman filter [163], T-f decomposition [160,164], HHT [165], etc. Other than harmonics in the phase currents, harmonics in dq currents are also evaluated for PD detection in [166].

The capability of certain harmonics to distinguish PD from eccentricity is paid special attention. In [159], the 2/3rd and 4/3rd harmonics emerge in the stator spectrum of a six-poles SPMSM under both the PD and dynamic eccentricity fault conditions, thus being unable to distinguish them. On the other hand, the 1/4th and 1/2nd harmonics are found able to distinguish PD from static eccentricity [167] in a nine-slot, eight-pole SPMSM. Amplitude and phase angle of the (1-1/p)f_e harmonics are used together to distinguish the PD and eccentricity faults. Furthermore, Naderi et al. [26] systematically analyze the homopolar frequency components in the stator current and conclude the components with the capability to distinguish between PD, eccentricity, and the ITSC fault.

The PD-related frequency components are studied comprehensively in [158,168], considering pole-slot combination, double-layer and single-layer winding, as well as skew angle. It is found that the harmonics at a triple multiple of mechanical frequency may disappear due to the winding configuration. Specifically, in the case when the following criteria are satisfied:

$$n_{layer} \times \frac{n_{slot}}{2p} = 3k, k = 1, 2, 3, \cdots,$$

PD does not create harmonics in stator currents, where n_{layer}, n_{slot}, and p are the number of winding layers, slots, and pole-pairs, respectively. A systematic analysis is presented in [169] about the harmonics in back-EMF under the PD and eccentricity conditions.

Apart from harmonics, the variation of the current angle [44] and torque angle [45] are found feasible to distinguish PD and ITSC faults, and, furthermore, the torque angle can be combined with the voltage vector amplitude to further discriminate PD, SE, and ITSC faults [43].

Methods based on current spectrum, Park's vector approach (PVA), and extended Park's vector approach (EPVA) are compared in [170] and the EPVA is found superior in terms of high sensitivity and robustness.

Furthermore, the signatures in the fifth harmonics subspace voltage vector of the DTPPMSM are investigated [171].

(c) HF pattern

Generally, very few papers utilize the HF pattern in voltages or currents for PD detection. However, it is found in [172] that the demagnetization can change the saturation level of the machine, and thus, it can be detected by inspecting the d-axis incremental inductance. It is also claimed that this method can detect PD faults in the case where machine current signature analysis (MCSA) cannot.

(d) Others

Instead of using spectrum analysis, Hong et al. [173] use the waveform of currents to detect PD at a standstill condition, essentially utilizing the impact of PD on the saturation level of the iron core. It is also worth mentioning that Fernandez et al. [174] and Reigosa et al. [175] managed to utilize the magnetoresistance effect of PM to estimate the magnetization state of PM.

3.2.2. Magnetic Signals

(a) Invasive methods

As discussed previously [158], some PD signatures in currents or voltages may not emerge depending on the topology of PMSM. Magnetic signal-based methods can get around that limitation by extracting the fault signatures directly from the flux or flux density.

The radial airgap flux density is analyzed at different working conditions in [176], and Hall sensors are placed in the airgap to obtain the corresponding signatures. Search coils wound on each tooth are adopted in [72], and the first-order harmonics amplitudes in each search coil are used. This method is improved in [177] by introducing a more robust fault index, which subtracts the average value of induced voltage in the range of a 120° mechanical angle from the original induced voltage waveforms. Multiple harmonics are used to evaluate the severity of PD in [178]. The abovementioned methods require search coils with only one tooth pitch wound on each tooth, which might be too complicated for a PMSM with many slots.

A method [179] is proposed by using two search coils placed on the tooth and facing the airgap. Four search coils are placed at the slot opening in [180]. In [181], six search coils with one pole pitch are placed in stator slots of a 36-slot, 4-pole machine. The induced voltage in the search coils is found to contain $(2k + 1 \pm 2/p)$th order harmonics when PD occurs. Rafaq et al. [182] find out that, for PD detection, only one search coil on the tooth is essentially enough because the demagnetized PM can be continually scanned by the search coils when the rotor is rotating. Skarmoutsos et al. [183] place a search coil in slots with the coil pitch being exactly a four-pole pitch. Consequently, the induced voltage will be zero under the healthy condition, resulting in a better signal-to-noise ratio (SNR). When PD occurs, the peak-to-peak value of induced voltage is used to calculate the fault index.

In addition, in [184], the search coils are wound at the stator yoke. Two search coils are placed at the bottom of two slots, whose distance is exactly one pole-pitch, and connect with each other in a way to make sure the ideal output is zero under the healthy condition.

Chen et al. [185] improved this method by adding another search coil, which is also one pole-pitch away. In total, eight search coils on the stator yoke are used in [74] to achieve discrimination between the PD and ITSC faults. Furthermore, the search coil on the rotor is also investigated in [186].

In [187], a special type of demagnetization was discussed, where the trailing edge of PM is demagnetized. It is demonstrated that monitoring airgap flux has the detectability of this type of demagnetization.

(b) Less invasive methods

The stray flux at the stator back side contains similar harmonics and signatures as the airgap flux [80,188]. Goktas et al. [189] apply two flux-gate sensors located behind the tooth and behind the slots, respectively. A circumferentially equidistant array of eight TMR sensors are placed outside the stator in [190]. The time domain fault index based on the envelope and the average of the stray flux density is calculated, which shows better performance than methods based on machine current signatures.

The stray flux in the end region can also be utilized. Hall sensors placed at the end region close to the PM are used to detect demagnetization [191]. The method is improved in [192] using the ZSC flux in the end region, which presents higher sensitivity. Park et al. [193,194] reduce the number of Hall sensors to one and further discuss the feasibility of fault detection with digital Hall sensors. The basic principle is that, if the rotor PMs are not symmetrical due to local demagnetization or damage, the flux measurement of the Hall sensor will be smaller when the demagnetized PM passes the Hall sensor.

3.2.3. Other Signals

PD causes harmonics in the spectrum of currents and voltages, consequently causing harmonics in torque, i.e., torque ripple. In [195], the amplitude of $(\lambda \pm \xi/p)$th harmonic in torque is chosen as the fault index, where λ and ξ are integers and p is the pole-pair number. Furthermore, the 0.25th harmonic in the vibration signal is used in [196].

3.2.4. Summary

Table 7 concludes the general advantages and disadvantages of different kinds of signal-based methods discussed in this section. Table 8 summarizes some of the typical research, its contributions, and aspects for further improvements.

Table 7. Comparison among signal-based methods of PD detection.

Signal Types	Fault Signature Types		Advantages		Disadvantages
Electrical signals	Symmetrical components	ZSC	+ Irrelevant to winding topology or machine topology	-	Difficult to measure
	Frequency pattern	Spectrum	+ Non-invasive	-	Highly dependent on winding topology and machine topology
		Impedance	+ High SNR	-	Highly influenced by temperature
	Others	Waveform pattern	+ Intuitive and simple	-	Highly influenced by saturation

Table 7. *Cont.*

Signal Types	Fault Signature Types		Advantages	Disadvantages
Magnetic signals	Invasive	All tooth mounted	+ Distinguishable among different faults + Intuitive	- Large amount of sensors
		Few teeth mounted	+ Fewer sensors	- Relatively difficult to distinguish PD from other faults
		Pole-specific search coils		
	Less invasive	Stator back side	+ Less invasive	- Affected by housing
		End region		- Difficult to accurately mount the sensors

Table 8. Typical works among signal-based methods for PD detection.

	Typical Works	Solved Problems	Unsolved Problems	Primarily Challenges
Electrical signals	[168]	Analysis considering machine topologies	Lacking universal detection methods	Extending the generalizability of electrical harmonics-based methods
Magnetic signals	[182]	Reduction in number of search coils	Non-stationary working conditions	Non-stationary working conditions

3.3. Model-Based Methods

The classification of model-based methods for PD detection is shown in Figure 11.

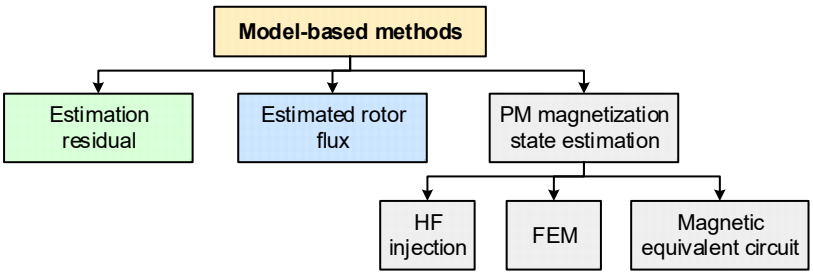

Figure 11. Classification of model-based methods for PD detection.

3.3.1. Estimation Residual

In [197], the airgap flux density is estimated in real-time through the analytical equations assisted with an offline FEM model and compared with the measured signal obtained with Hall sensors. The deviation is then processed with a wavelet transform to extract the target frequency, followed by a classifier. Bisschop et al. [198,199] managed to build up the analytical expression of the induced voltage in search coils. Then, the predicted induced voltage is compared with the measured value, and the deviation is used to evaluate the severity of PD.

3.3.2. Estimated Rotor Flux

Roux et al. [200] estimated d-axis flux linkage with the voltage equation of PMSM and monitored the decreases in the estimated value. Moon et al. [201] present a method to estimate the PM flux and the L_d and L_q at the same time. The variation in PM flux is combined with the deviation of L_d and L_q to detect PD. Zhu et al. [202] estimate the rotor flux by using torque ripple as the input of the rotor flux estimation algorithm. Liu et al. [203] also estimate the rotor flux while simultaneously monitoring the HF d-axis inductance to discriminate the eccentricity and the PD faults. Han et al. [204] further take

the variation of parameters into consideration and successfully separated the estimated quantity irrelevant to parameter error. Rotor flux linkage can also be estimated with PWM voltage measurements [205] to exclude the influence of inverter nonlinearity.

For DTPPMSM, PD detection can be achieved by monitoring the flux linkage in the fifth harmonics subspace [206].

3.3.3. PM Magnetization State Estimation

Demagnetization is essentially the change of the PM magnetization state. Hence, monitoring the PM magnetization state can detect the PD fault. FEM is one of the most common techniques to evaluate the magnetization state of the PMs [207–209]. However, the high computational burden of FEM makes it almost impossible for online detection. Therefore, a magnetic equivalent circuit is adopted in [168,210,211] to replace the FEM.

3.3.4. Summary

Table 9 concludes the general advantages and disadvantages of different kinds of model-based methods discussed in this section. Table 10 summarizes some of the typical research, its contributions, and aspects for further improvements.

Table 9. Comparison among model-based methods of PD detection.

Signal Sources	Signatures	Advantages	Disadvantages
Voltage/Current	Estimated rotor flux	+ Non-intrusive + Suitable for transient condition	- Unable to locate fault - Low sensitivity - Essentially influenced by machine topology
Flux signal + Voltage/current	Estimation residual	+ High sensitivity	- High cost of flux sensors - Invasive
Voltage/Current	PM magnetization state estimation	+ Non-intrusive	- Generally high computational burden

Table 10. Typical works among model-based methods for PD detection.

Typical Works	Solved Problems	Unsolved Problems	Primarily Challenges
[203]	Distinguish between PD and eccentricity	Influence of saturation level is not thoroughly analyzed	Elimination of load conditions

3.4. Data-Based Methods

The classification of data-based methods for PD detection is shown in Figure 12.

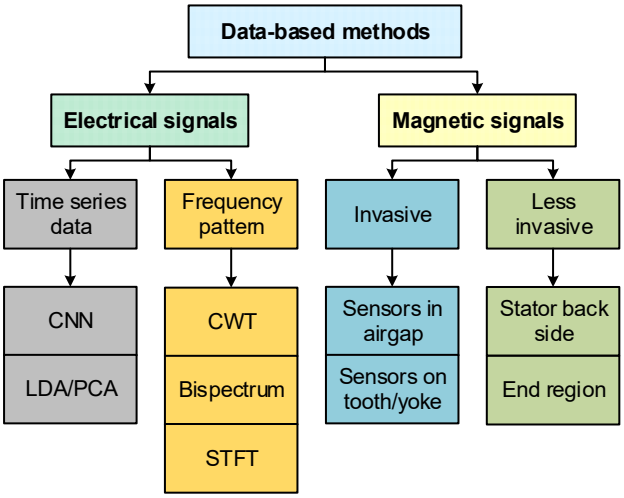

Figure 12. Classification of data-based methods for PD detection.

3.4.1. Electrical Signals

Skowron et al. [212] target detecting the ITSC fault and the PD fault at the same time. The raw current signals are constructed as a 20 × 25 × 3 array and fed into a CNN. A similar principle is adopted in [213], while a transfer learning technique is integrated into the diagnosis framework. Chen et al. [147] also adopted CNN to distinguish ITSC and PD but processed the current and voltage signals with a model-based method and fed the CNN with a q-axis current residual. Other than CNN, linear discriminant analysis and principal component analysis are combined with a variational autoencoder in [74] to extract implicit features in current signals.

The method proposed in [214] converts both voltage and current signals into images and then processes them with a local binary pattern texture analysis. The extracted features are then classified using a KNN algorithm. Bispectrum is adopted to convert the three-phase currents into images in [215] to detect eccentricity and PD faults. Continuous wavelet transform (CWT) is combined with ResNet in [119], and the short-time Fourier transform (STFT) is combined with KNN and a multilayer perceptron in [216]. The combination of signal-based methods and data-based methods enhances the robustness of detection methods against transient processes.

It is worth noting that, because of the strong capability of machine learning algorithms, a lot of papers investigate the discrimination among different fault types based on voltage and current signals, such as ITSC and PD [119,143,147,217,218], eccentricity and PD [215,217,219,220], etc.

Since the demagnetization of PM is sensitive to temperature, the influence of PD on machine temperature is analyzed in [221], and the temperatures of the shell and winding are used in addition to current, torque, and speed signals.

3.4.2. Magnetic Signals

In [222–224], airgap flux density is measured with three gauss meter probes located in different positions in the airgap of a double-side linear PMSM. In [222], complex CWT and the Teager–Kaiser energy operator are used to extract the fault feature, while in [223], a time–time transform is used. Random forest and an extreme learning machine are adopted as classifiers, respectively. Other than using flux density measuring sensors, search coils wound on tooth [148] and yoke [225] are also adopted to capture the distortion in the airgap flux density.

In [226], a stray flux signal sampled outside the stator back-iron is converted into a symmetric dot pattern image and analyzed by a wavelet scattering convolution network and semi-supervised deep rule-based classifier. Similar stray flux sensors are placed in [227], while the sampled signals are processed with the local outlier filter and deep Q-network.

3.4.3. Summary

Table 11 concludes the general advantages and disadvantages of different kinds of data-based methods discussed in this section. Table 12 summarizes some of the typical research, its contributions, and aspects for further improvements.

Table 11. Comparison among data-based methods of PD detection.

Signal Sources		Advantages				Disadvantages			
Electrical signals	Voltages and currents	+	Non-invasive	+	Suitable for multi-sensor fusion High sensitivity	-	Influenced by machine topology	-	High computational burden
Magnetic signals	Airgap flux	+	Universal			-	Need extra sensors		
	Stray flux	+	Less invasive						
Others	Torque	+	Non-invasive						
	Acoustic noise								

Table 12. Typical works among data-based methods for PD detection.

Typical Works	Solved Problems	Unsolved Problems	Primarily Challenges
[216]	Combination of signal-based and data-based methods and improvement in transient conditions	Influence of noise and sampling rate	Improve robustness against noise in collected data

4. Eccentricity Detection

4.1. Background

Eccentricity refers to the misalignment of the geometrical center of the rotor and stator, resulting in an unevenly distributed airgap. Many factors can cause eccentricity, such as manufacturing tolerance, bearing faults, rotor deformation, etc. Generally, there are three types of eccentricity, including static eccentricity (SE), dynamic eccentricity (DE), and mix eccentricity (ME).

SE occurs when the rotating center of a rotor is not aligned with the center of stator O_s while being aligned with the geometric center of rotor O_r. As shown in Figure 13a, SE results in an unevenly distributed but time-invariant airgap.

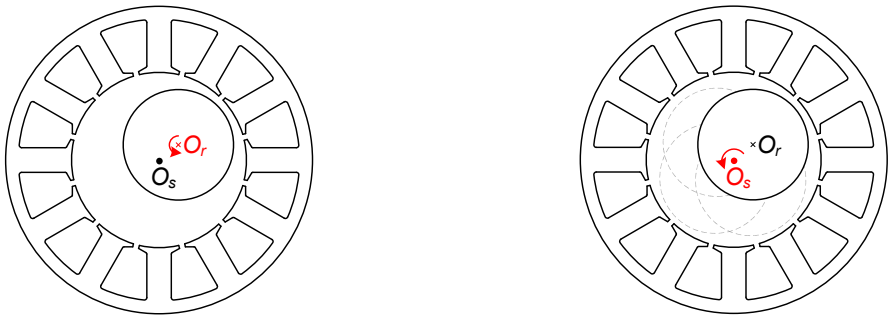

(**a**) (**b**)

Figure 13. Illustration of eccentricity. (**a**) SE; (**b**) DE.

On the other hand, DE means the rotating center of a rotor is aligned with the center of stator O_s but misaligned with the geometric center of rotor O_r. It can be seen from Figure 13b that the position of the minimum airgap rotates with the rotor, but the average airgap length is still the nominal airgap length.

ME is essentially the mixture of SE and DE.

With an uneven airgap, eccentricity causes harmonics in back-EMF [228] and currents, torque ripple, the unbalanced magnetic pull (UMP) [229], and vibration [230]. It is also reported in [231] that eccentricity has a very significant influence on cogging torque in machines having $2p = N_s \pm 1$, where p is the pole-pair number and N_s is the number of stator slots.

4.2. Signal-Based Methods

The classification of signal-based methods for eccentricity detection is shown in Figure 14.

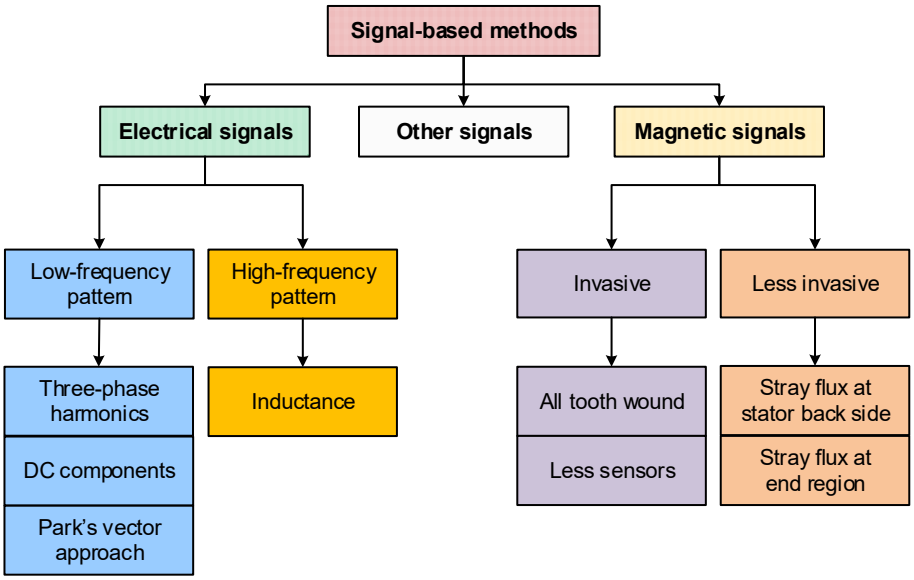

Figure 14. Classification of signal-based methods for eccentricity detection.

4.2.1. Electrical Signals

(a) LF pattern

Fractional harmonics are commonly observed in stator currents and voltages when an eccentricity fault occurs. The harmonics caused by DE can be expressed as [159,232]

$$f_{de} = f_e\left(1 \pm \frac{2k-1}{p}\right),\ k = 1, 2, 3, \cdots. \tag{2}$$

Meanwhile, the $(1 + 2k/p)$th harmonics are found related to SE in [232] for the studied machine.

For DE detection, the 2/3rd and 4/3rd harmonics of a six-poles BLDC are analyzed and tracked with a windowed Fourier transform [9], analytical wavelet transform [233], and the quadratic time-frequency representation method [234]. Meanwhile, frequency components with even multiples of mechanical frequency harmonics are selected as fault indicators for DE in [27] and are found to be able to distinguish DE from ITSC faults. Discrimination of DE from PD is accomplished in [235] based on the amplitudes and phase angles of monitored harmonics. IPMSMs and SPMSMs are compared in [236] and found no impact on the existence of the harmonics. Similar frequency components are obtained in [237] through synchronous resampling to obtain better consistency at various operation conditions.

For SE detection, the 1/4th harmonics is selected of a nine-slot, eight-pole SPMSM in [167]. Skarmoutsos et al. [238] propose an algorithm to analytically calculate the fractional harmonics that exist in phase voltage and point out that the coil and pole number can influence the harmonic existence expressed in (2). It is also discovered in [228] that the back-EMF is not affected by eccentricity in rotationally symmetrical machines, leading to a reduction in fault harmonics.

Integer harmonics also emerge when an eccentricity fault occurs. In [200], the NSC of the seventh harmonic in currents is chosen as the fault indicator for SE. The fundamental frequency component in the ZSVC difference between two sets of windings in a DTPPMSM is used for SE detection in [239], while the sideband $(1 \pm 1/p)^{\text{th}}$ harmonics are used for DE detection.

As mentioned in the methods of ITSC and PD faults, the variation of fundamental frequency components is used in [43] to discriminate ITSC, PD, and SE. Back-EMF at

various speeds and speed-fluctuation conditions is collected and used for DE detection in [240].

(b) HF pattern

HF pattern can reflect the changes of inductance due to the fault. It is pointed out that variation in the PM flux results in the saturation degree in the *d*-axis and thus changes the *d*-axis inductance [241]. A pulsating voltage at the *d*-axis is injected under the standstill condition to calculate the *d*-axis inductance and, consequently, to detect SE. The method is further extended [172] to non-standstill conditions and enabled to discriminate demagnetization and DE. A DC voltage in the *d*-axis is further injected, superimposed with a pulsating HF voltage, and incremental inductance is calculated with the response current. The increase and decrease in inductance compared with a healthy machine are used as features for demagnetization and eccentricity faults. Furthermore, Liu et al. [203] utilize the mechanical frequency fluctuation of *d*-axis inductance to detect DE. Similarly, Aggarwal et al. [242] propose an off-line test method based on incremental inductance, while another criterion is added, that is, the hump height of the inductance curve versus the current.

4.2.2. Magnetic Signals

Similar to the PD fault, the eccentricity fault features may be influenced by the machine topology [228,238]. In comparison, the magnetic signals directly monitor the field distribution without relying on the signals filtered by the phase windings. Thus, magnetic signals have a significant advantage of universality in the detection of eccentricity.

(a) Invasive methods

Search coils wound on each tooth are feasible for detecting both SE and DE and also able to distinguish them from each other [72,177,182]. In [177], two specially designed fault indicators are calculated from the induced voltages to separately distinguish PD and eccentricity faults. Meanwhile, the nominal peak values of the induced voltages are used as fault indicators in [182]. Furthermore, only one search coil in [243] is placed in the slots, whose coil pitch is about the even multiple of the pole-pitch, so that the induced voltage can be eliminated under the healthy condition. In [244], Hall sensors are placed at the slot opening. The NSC and the single side-band components in the flux density are used as the fault signatures of the SE and DE, respectively.

(b) Less invasive methods

Sensors are mounted onto the stator back side of a synchronous generator to capture the stray field [245,246] and manage to distinguish the SE and DE. An analytical method is developed in [247] to predict the stray flux at the stator back side under the SE condition. Hall sensors are mounted at the end region in [194,248] to capture the distortion due to eccentricity. In [248], the RMS of induced voltages is compared among the four search coils. It is proved that the digital Hall sensor is also feasible as a cheaper alternative to the analog Hall sensor [194].

4.2.3. Other Signals

Cogging torque is found to contain signatures of eccentricity in [249,250]. It is also stated in [251] that, by measuring the UMP, discrimination can be achieved between SE and DE. Furthermore, the vibration and acoustic noise caused by eccentricity is investigated in [252] and [253], respectively.

In [254], the temperature asymmetry of the whole machine is utilized for SE detection. The asymmetry in iron loss distribution is discovered when SE exists, resulting in the asymmetry of temperature.

4.2.4. Summary

Table 13 concludes the general advantages and disadvantages of different kinds of signal-based methods discussed in this section. Table 14 summarizes some of the typical research, its contributions, and aspects for further improvements.

Table 13. Comparison among signal-based methods of eccentricity detection.

Fault Signature Types			Advantages		Disadvantages
Electrical signals		Voltage/Current spectrum	+ Non-invasive	-	Dependent on winding topology/machine topology
		Impedance	+ Less influenced by machine topology	-	Highly sensitive to working conditions
Magnetic signals	Invasive	All tooth wound	+ High sensitivity	-	Need a lot of sensors
		Fewer sensors	+ Relatively low cost	-	Invasive
	Less invasive	Stator back side		-	Influenced by housing
		End region	+ Less invasive	-	Need accurate position of search coils

Table 14. Typical research among signal-based methods for eccentricity detection.

	Typical Works	Solved Problems	Unsolved Problems	Primarily Challenges
Electrical signals	[241]	Improvement in simplicity and generalizability	Unable to online monitor	Continuous monitoring accounting for variation of working conditions
Magnetic signals	[72]	Generalizability among different kinds of PMSMs	Large number of sensors	Reduction in the number of search coils

4.3. Model-Based Methods

According to the criteria adopted in this paper, very few methods for eccentricity detection are classified as model-based methods. Thus, this category of methods is omitted here.

4.4. Data-Based Methods

Classification of data-based methods for eccentricity detection is shown in Figure 15.

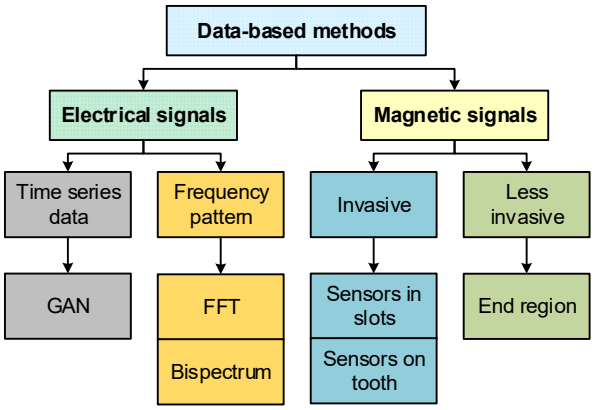

Figure 15. Classification of data-based methods for eccentricity detection.

4.4.1. Electrical Signals

Ebrahimi et al. [232] extract the sideband frequency components from stator currents, and the KNN classifier is cascaded with an artificial neural network (ANN) to distinguish SE, DE, and ME. Furthermore, in [255], the fault features of SE and DE are extracted from the

harmonics around the fundamental frequency component and classified with SVM. Similar harmonics are used in [256], while the harmonics are obtained with wavelet analysis. The classification is achieved with KNN, and the evaluation of severity is achieved with SVM. In [215], three-phase currents are processed with bispectrum analysis and converted into images. Specifically, the information in different frequency ranges is separately extracted and transformed into images to minimize the invalid information for ME detection.

In [217], the time and frequency indices are calculated with *dq* currents and fed into different outlier detection methods, including isolation forest, SVM, and robust covariance ellipse. The results of these methods are ensembled by majority voting ensemble techniques.

The eccentricity fault in DTPPMSM is analyzed in [220]. The voltage angle increases under SE conditions compared with healthy conditions. Thus, the voltage angle is then processed with a multivariate regression analysis and ANNs for fault classification.

A method is proposed in [257] using a generative adversarial network (GAN) to solve the problem of data lacking for data-based eccentricity detection methods. GAN is employed to generate back-EMF data similar to the actual data, based on the data calculated from the analytical model. Furthermore, in [258], a new fault diagnosis framework is proposed where only healthy data is required. The GAN is used to combine the data provided by ideal mathematical and FEM models of PMSM with eccentricity and the actual data and eventually provides the accurate prediction of back-EMF at different eccentricity degrees.

4.4.2. Magnetic Signals

In [148], the ITSC, PD, SE, and DE can be successfully detected and separated based on the search coils wound on a tooth. The SqueezeNet is adopted to capture those fault features in the induced voltages that can distinguish these faults from each other.

In [219], six search coils placed in slots are used as the signal sources, and the amplitudes of the fractional harmonics in the induced voltage are classified based on random forest, achieving an accurate detection of DE and discrimination from PD.

In [259], the stray flux in the end region of a linear PMSM is collected with TMR sensors. The Gramian angular field and Markov transition field are used to convert 1D data into 2D images, which is then processed with fusion feature extraction algorithms and neural networks.

4.4.3. Summary

Table 15 concludes the general advantages and disadvantages of different kinds of data-based methods discussed in this section. Table 16 summarizes some of the typical research, its contributions, and aspects for further improvements.

Table 15. Comparison among data-based methods of eccentricity detection.

Fault Signature Types			Advantages		Disadvantages	
Electrical signals			+	Non-invasive	-	Dependent on winding topology/machine topology
Magnetic signals	Invasive	All tooth wound	+ +	High sensitivity Able to distinguish SE, DE, PD, and ITSC	- -	Need a lot of sensors Invasive
		Fewer sensors	+ +	Relatively low cost Able to distinguish DE from PD	-	Invasive
	Less invasive	End region	+	Less invasive	-	Low SNR

Table 16. Typical research among data-based methods for eccentricity detection.

Typical Works	Solved Problems	Unsolved Problems	Primarily Challenges
[257]	Generation of data to fulfill the requirement of the training dataset	Accounting for transient process	Generation of data considering transient conditions

5. Evaluation of Existing Methods

5.1. General Evaluation

Various kinds of detection methods are discussed in this paper. Table 17 evaluates these methods from four different perspectives, including the complexity, computational burden, accuracy, and generalizability.

Table 17. Evaluation of detection methods based on different metrics.

Categories	Signature Types	Complexity	Computational Burden	Accuracy	Generalizability
Signal-based	Sequence components	Low	Low	Low	ITSC: High
	LF harmonics-based	Low	Low~Medium	Medium	PD, SE, DE: Low
	HF patterns	Medium	Low	Medium	Medium
	Main flux signals	High	Low	High	High
	Stray flux signals	Medium~High	Low	Medium	Medium
Model-based	Estimation residuals	Medium	Medium	Low~Medium	Medium
	Estimated fault parameters (SC ratio, rotor flux, etc.)	Medium	Medium	Low	ITSC: Medium PD, SE, DE: Low
Data-based	-	Medium~High	High	High	Medium

Combining the information shown in Table 17 and the discussion in previous sections, generally speaking, the strengths and the weaknesses of different methods can be concluded as follows:

Signal-based methods have the advantages of simplicity and low computational burden. Meanwhile, compared with model-based methods, their dependency on the machine parameters is relatively minor. However, they struggle with the non-stationary conditions, which can be mitigated with specific analysis tools such as EMD or HHT at the cost of higher complexity and computational burden.

Model-based methods are naturally suitable for monitoring under non-stationary conditions. However, its dependency on the accuracy of machine parameters has been a challenge.

On the other hand, data-based methods can achieve very high sensitivity and accuracy compared to the other two categories of methods. Meanwhile, the self-adaptive learning feature enables the automatic diagnosis process [3], reducing interference from humans. Furthermore, the capability of representing high-dimensional nonlinear relationships between the fault features and practical conditions provides better performance in various operating conditions. However, the requirement of historical data is very difficult to fulfill in some cost-sensitive cases, as well as the high computational resources needed.

It is also worth noting that, for ITSC faults, the machine topologies have little effect on the harmonics in electrical signals. However, for rotor faults, i.e., PD, SE, and DE, the information in electrical signals is highly related to machine topologies. On the other hand, magnetic signals, especially the flux signals on the main flux path, can contain signatures related to ITSC, PD, SE, and DE. Consequently, magnetic signal-based methods can have the best generalizability. Also, the airgap flux profile provides fault-related information without the influence of machine topologies. Hence, by analyzing the airgap flux profile, such as methods based on search coils wound on all the teeth [72,148] and Hall sensors placed in the airgap [222–224], the scalability of these methods can be promisingly ensured.

5.2. Challenges and Gaps in Existing Methods

5.2.1. Signal-Based Methods

For the method using low-frequency patterns in electrical signals, one of the major challenges lies in avoiding the false alarm caused by the transient process. This problem can

be mitigated by adopting non-stationary signal analysis tools during transient processes or even simply disabling the detection algorithms during transient processes.

Meanwhile, the HF frequency patterns can also resist the influence of transient processes. But to obtain HF patterns, HF signals must be extracted, which usually means undesirable noises and a reduction in efficiency. The methods using PWM ripple currents further require additional sampling boards because the switching frequency patterns must be sampled at a very high sampling rate, resulting in extra costs and complexity.

The magnetic signal-based methods generally have a better SNR, but they have to confront a problem, i.e., the placement of flux sensors. The sensors in the airgap, slots, or yoke can have very good sensitivity to faults, but they may also be damaged by the faults in the machine. On the other hand, the stray flux sensors in the end region or stator back side suffer from the noise and uncertainty from other components such as end plates and housings.

5.2.2. Model-Based Methods

It is known that the accuracy of model-based methods is highly dependent on the accuracy of the adopted model. However, PMSM drive systems are highly nonlinear due to the magnetic properties of the iron cores and the characteristics of the switching devices. Hence, when applied to practical systems, the model-based methods must take into account the variation of the PMSM model at different working conditions.

In most existing model-based methods, the proposed fault indicators are derived with the assumption of only one fault. This leads to another challenge of model-based methods, which is that they generally lack the capability to distinguish between different kinds of faults. In particular, the model-based methods estimating the fault parameters, e.g., the short-circuit ratio or the rotor flux, require the faulty PMSM models, and thus the complexity and the computational burden increase drastically when considering multiple faults. On the other hand, the methods based on estimation residuals only need the healthy PMSM model, and hence, in theory, they can be easily adapted to detect and distinguish multiple faults, according to the patterns in the residuals. Nevertheless, for now the capability of model-based methods on identifying multiple faults has not been widely investigated yet.

5.2.3. Data-Based Methods

In practical applications, data-based methods mainly face two challenges, i.e., the need for historical data and the high demand for computational resources. For most of the machine learning algorithms, the quality of the collected data is very important, whereas those deep learning algorithms further require a sufficient amount of historical data. A large number of experiments must be accomplished to obtain enough historical data, which is very challenging for cost-sensitive or high-power occasions. Meanwhile, to ensure the quality of collected data, pre-processing progress is also vital. As referred to in this review, some researchers are attempting to tackle this problem by using GAN as well as FEM models, but further investigation is still required to address this problem.

The demand for computational resources is high because data-based methods usually need many parameters to take part in the calculation to account for the high-dimensional information in historical data. Hence, the calculation process takes a lot of time, and the storage of these parameters consumes a large amount of memory. This can be extremely challenging when applied to embedded systems.

Furthermore, the generalizability, i.e., the feasibility, of applying certain data-based methods to different kinds of PMSMs is questionable. In most existing research, the historical data is collected and tested on one or several typical prototypes while lacking

testing on other kinds of prototypes. This problem is usually minor in signal- and model-based methods because the fault modeling techniques are very mature, with which it is normally predictable whether the fault signatures will emerge in certain kinds of PMSMs. However, the lack of interpretable information in machine learning algorithms, especially deep learning algorithms, prevents users from predicting the generalizability of data-based methods.

5.3. Applicability in Industrial Applications

In industrial applications, the feasibility of a fault detection method is related to multiple factors, including their capability, cost, hardware requirements, etc. Obviously, different industrial settings have different thresholds for these factors, and therefore it is important to evaluate them case by case when selecting the detection methods. Here, two typical industrial applications are discussed, i.e., electrical vehicles and wind power generation.

5.3.1. Electric Vehicle Applications

Electric vehicles are known for their high demand for enhancing safety and reducing cost. In electrical vehicles, the speed of the drive machine is usually varying during most of its operation time. In such cases, it is difficult to collect a period of stationary data, limiting the capability of traditional signal-based methods such as sequence-component-based methods.

On the one hand, offline tests can be a universal solution, but they cannot meet the instant interference requirement, and thus they usually cannot prevent an escalation during the operation. On the other hand, this difficulty can be mitigated with non-stationary signal analysis tools, such as EMD and STFT, or with model-based methods. Compared to the signal-based methods with non-stationary signal analysis tools, one of the advantages of model-based methods is that they can easily evaluate the fault severity on which the fault-tolerant control is based. As for data-based methods, balancing between the required computational resources and the additional costs is troublesome for now. Hence, the model-based methods seem more preferable in electrical vehicle applications. However, with the growth of computational resources in electrical vehicles, data-based methods will become more and more feasible in the future due to their high sensitivity and capability of detecting multiple faults.

It is worth noting that high-frequency injection is also capable of eliminating the influence of varying speeds, but the harsh noise and extra vibration it brings are generally unwanted in electrical vehicles.

5.3.2. Wind Power Generation Applications

Due to the fact that wind power generators usually have high-rated power, a huge number of poles and slots, and a high number of parallel branches, the fault signatures of an early-stage fault are usually very small. For wind power generation applications, the major concern when choosing fault detection methods becomes the sensitivity to the faults as well as the cost, and it is vital to find the balance between high detection sensitivity and the cost.

Computational resources are usually more adequate for wind power generators compared to electrical machines in electrical vehicles, considering that the wind power generators are fixed in one position and with adequate electricity input from the mains. Hence, in such cases, data-based methods are usually preferred. Obviously, data-based methods can achieve a very high sensitivity with the proper amount of historical data. Also, these methods have very strong capabilities to detect and identify different kinds of faults. Thus, compared with other kinds of methods, data-based methods are easier to be integrated into a systematic fault diagnosis system.

From the perspective of signal sources, it should be noted that the magnetic-signal-based methods are very difficult to implement in a wind power generator because the generators usually have large amounts of poles and slots, causing numerous extra sensors and enormous complexity. However, it is worth noting that the methods using a stray flux at the stator back side, such as in [245,246], have been applied to large synchronous generators, showing their potential to be applied to wind power generators.

6. Discussion

6.1. Signal-Based Methods

The ITSC, PD, SE, and DE all introduce unwanted harmonics in currents but with different frequencies. However, the PD, SE, and DE fault-related harmonics are much more sensitive to the machine topology compared to the ITSC fault. This is because the windings act as filters to the harmonics introduced by rotor faults. In contrast, it is more difficult for the windings to filter through the harmonics caused by the faults in themselves. Consequently, it can be observed that magnetic signals have higher SNR and better universality for rotor fault detection.

6.2. Model-Based Methods

The model-based methods are much more popular in the area of ITSC fault detection than the other two. This could be due to the phenomenon stated before, that is, in some cases the information in the stator currents and voltages is not enough.

6.3. Data-Based Methods

Data-based methods have gained more and more attention in recent years. It can be observed that the recent trend in data-based methods is integrating multiple types of signals, i.e., sensor fusion, and distinguishing different kinds of faults. These tasks are very difficult for traditional techniques due to the highly non-linear and uncertain relationship between the fault signatures and the faults, especially in practical applications. However, since machine learning algorithms, especially those deep learning algorithms, have very strong representation capabilities, this relationship can possibly be learned with enough data and the appropriate algorithms.

7. Conclusions and Future Work

The state-of-the-art techniques of the fault detection methods of PMSMs are comprehensively reviewed in this paper. Three major faults are covered, i.e., the ITSC fault, the PD fault, and the eccentricity fault. The existing methods are classified into signal-, model-, and data-based methods and further categorized according to the signal types they used. Then, the existing methods are discussed in detail, and special attention is paid to the fault signatures they use. Subsequently, a comparison is conducted between methods with different signal sources and fault signatures, as well as the methods for the three types of faults. Generally speaking, signal-based methods are relatively simple and have a low computational burden, though they find it difficult to suppress transient false alarms. Model-based methods are more suitable for transient working conditions, but at the cost of a higher computational burden and lower SNR. Data-based methods are the hottest topic in recent years. They have advantages of a high SNR and strong capabilities in distinguishing different faults. But the computational burden is usually very high.

According to the discussions and analyses in this paper, various directions for future work can be pointed out, as shown in Figure 16.

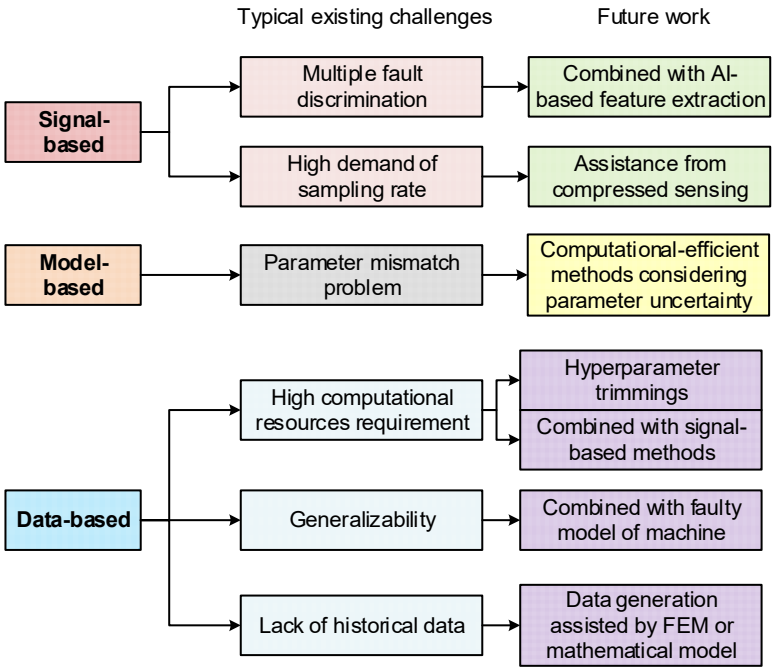

Figure 16. Illustration of existing challenges and future work.

In particular, future research can be initiated in the following directions, which are difficult but very promising:

(1) Implementation of data-based methods in real-time systems and embedded systems. This means that sufficient improvements need to be accomplished in the computational efficiency of the data-based methods.
(2) Sensor fusions. Sensor fusion can be an important approach to enhance the sensitivity and generalizability of fault detection methods, but it must overcome difficulties in processing large amounts of data with various specifications, such as sampling rate and data range, etc.
(3) Improving the capability of distinguishing different faults. It has been widely investigated how to distinguish different faults, while very few methods with good universality are developed.
(4) Detection of faults in DTPPMSM. Compared with traditional three-phase PMSMs, DTPPMSMs have more control degrees, and also more sampled current signals. Thus, potentially higher SNR can be achieved.

Author Contributions: Conceptualization, Z.-Q.Z. and H.L.; methodology, Z.-Q.Z. and H.L.; formal analysis, H.L.; investigation, H.L.; resources, Z.-Q.Z.; writing—original draft preparation, H.L.; writing—review and editing, Z.-Q.Z., Z.A., R.C. and Z.W.; supervision, Z.-Q.Z., Z.A., R.C. and Z.W.; project administration, Z.-Q.Z.; funding acquisition, Z.-Q.Z. and Z.A. All authors have read and agreed to the published version of the manuscript.

Funding: This work was supported by the Siemens Gamesa Renewable Energy A/S, Denmark, under Grant No. R/173973-11-1.

Data Availability Statement: Not applicable.

Conflicts of Interest: The authors declare that they have no conflicts of interest. The funder had no role in the design of the study; in the collection, analyses, or interpretation of data; in the writing of the manuscript; or in the decision to publish the results.

Acronyms

AI	Artificial intelligence	MMF	Magnetomotive force
ANN	Artificial neural network	NSC	Negative sequence component
BLDC	Brushless DC	PD	Partial demagnetization
CNN	Convolutional neural network	PLL	Phase lock loop
CWT	Continuous wavelet transform	PM	Permanent magnet
DE	Dynamic eccentricity	PMSG	PM synchronous generator
DTPPMSM	Dual three-phase PMSM	PMSM	PM synchronous machine
DWT	Discrete wavelet transform	PSC	Positive sequence component
EMD	Empirical mode decomposition	PVA	Park's vector approach
EMF	Electromotive force	PWM	Pulse width modulation
EPVA	Extended Park's vector approach	RMS	Root mean square
FEM	Finite element method	RNN	Recurrent neural network
FFT	Fast Fourier transform	SE	Static eccentricity
GAN	Generative adversarial network	SNR	Signal-to-noise ratio
HF	High frequency	SPMSM	Surface-mounted PMSM
HRC	High resistance connection	STFT	Short-time Fourier transform
IPMSM	Interior PMSM	SVPWM	Space vector PWM
IRP	Instantaneous reactive power	TMR	Tunnelling magneto-resistive
ITSC	Inter-turn short-circuit	UD	Uniform demagnetization
KNN	K-nearest neighbor	UMP	Unbalanced magnetic pull
LF	Low frequency	VMD	Variational mode decomposition
LUT	Look-up table	ZSC	Zero sequence component
MCSA	Machine current signature analysis	ZSVC	Zero sequence voltage component
ME	Mixed eccentricity		

References

1. Zhu, Z.Q.; Howe, D. Electrical Machines and Drives for Electric, Hybrid, and Fuel Cell Vehicles. *Proc. IEEE* **2007**, *95*, 746–765. [CrossRef]
2. Zhang, P.; Du, Y.; Habetler, T.G.; Lu, B. A Survey of Condition Monitoring and Protection Methods for Medium-Voltage Induction Motors. *IEEE Trans. Ind. Appl.* **2011**, *47*, 34–46. [CrossRef]
3. Orlowska-Kowalska, T.; Wolkiewicz, M.; Pietrzak, P.; Skowron, M.; Ewert, P.; Tarchala, G.; Krzysztofiak, M.; Kowalski, C.T. Fault Diagnosis and Fault-Tolerant Control of PMSM Drives–State of the Art and Future Challenges. *IEEE Access* **2022**, *10*, 59979–60024. [CrossRef]
4. Pengbo, Z.; Renxiang, C.; Xiangyang, X.; Lixia, Y.; Mengyu, R. Recent Progress and Prospective Evaluation of Fault Diagnosis Strategies for Electrified Drive Powertrains: A Comprehensive Review. *Measurement* **2023**, *222*, 113711. [CrossRef]
5. Jiang, Y.; Ji, B.; Zhang, J.; Yan, J.; Li, W. An Overview of Diagnosis Methods of Stator Winding Inter-Turn Short Faults in Permanent-Magnet Synchronous Motors for Electric Vehicles. *WEVJ* **2024**, *15*, 165. [CrossRef]
6. Faiz, J.; Bazrafshan, M.A.; Tabarniarami, Z. Demagnetisation Fault Analysis and Diagnosis Based on Different Methods in Permanent Magnet Machines—An Overview. *IET Electr. Power Appl.* **2024**, *18*, 1860–1893. [CrossRef]
7. Faiz, J.; Nejadi-Koti, H. Eccentricity Fault Diagnosis Indices for Permanent Magnet Machines: State-of-the-art. *IET Electr. Power Appl.* **2019**, *13*, 1241–1254. [CrossRef]
8. Solís, R.; Torres, L.; Pérez, P. Review of Methods for Diagnosing Faults in the Stators of BLDC Motors. *Processes* **2022**, *11*, 82. [CrossRef]
9. Rajagopalan, S.; Aller, J.M.; Restrepo, J.A.; Habetler, T.G.; Harley, R.G. Detection of Rotor Faults in Brushless DC Motors Operating Under Nonstationary Conditions. *IEEE Trans. Ind. Appl.* **2006**, *42*, 1464–1477. [CrossRef]
10. Grubic, S.; Aller, J.M.; Bin, L.; Habetler, T.G. A Survey on Testing and Monitoring Methods for Stator Insulation Systems of Low-Voltage Induction Machines Focusing on Turn Insulation Problems. *IEEE Trans. Ind. Electron.* **2008**, *55*, 4127–4136. [CrossRef]
11. Hang, J.; Zhang, J.; Cheng, M.; Huang, J. Online Interturn Fault Diagnosis of Permanent Magnet Synchronous Machine Using Zero-Sequence Components. *IEEE Trans. Power Electron.* **2015**, *30*, 6731–6741. [CrossRef]
12. Zhu, Y.; Cai, S.; Li, B. Detection and Discrimination of Interturn Fault and High-Resistance Connection Fault in PMSM Based on Deviation Angle of Zero Sequence Voltage. *IEEE Trans. Transp. Electrif.* **2024**, *10*, 7623–7632. [CrossRef]

13. Hang, J.; Ding, S.; Ren, X.; Hu, Q.; Huang, Y.; Hua, W.; Wang, Q. Integration of Interturn Fault Diagnosis and Torque Ripple Minimization Control for Direct-Torque-Controlled SPMSM Drive System. *IEEE Trans. Power Electron.* **2021**, *36*, 11124–11134. [CrossRef]
14. Hang, J.; Sun, W.; Hu, Q.; Ren, X.; Ding, S. Integration of Interturn Fault Diagnosis and Fault-Tolerant Control for PMSM Drive System. *IEEE Trans. Transp. Electrif.* **2022**, *8*, 2825–2835. [CrossRef]
15. Wang, H.; Wang, J.; Wang, X.; Lu, S.; Hu, C.; Cao, W. Detection and Evaluation of the Interturn Short Circuit Fault in a BLDC-Based Hub Motor. *IEEE Trans. Ind. Electron.* **2023**, *70*, 3055–3068. [CrossRef]
16. Laadjal, K.; Antunes, H.R.P.; Sahraoui, M.; Bento, F.; Marques Cardoso, A.J. On-Line Diagnosis and Discrimination of Stator Faults in Six-Phase Induction Motors, Based on Voltage Symmetrical Components. *IEEE Trans. Transp. Electrif.* **2022**, *9*, 3115–3126. [CrossRef]
17. Laadjal, K.; Bento, F.; Serra, J.; Cardoso, A.J.M. An Integrated Strategy for the Real-Time Detection and Discrimination of Stator Inter-Turn Short-Circuits and Converter Faults in Asymmetrical Six-Phase Induction Motors. *IEEE Trans. Ind. Appl.* **2023**, *60*, 377–387. [CrossRef]
18. Alloui, A.; Laadjal, K.; Sahraoui, M.; Marques Cardoso, A.J. Online Interturn Short-Circuit Fault Diagnosis in Induction Motors Operating Under Unbalanced Supply Voltage and Load Variations, Using the STLSP Technique. *IEEE Trans. Ind. Electron.* **2023**, *70*, 3080–3089. [CrossRef]
19. Wu, Y.; Zhang, J.; Xu, Z.; Wang, S.; Fu, H. Feature Extraction and Applicability Comparisons for Fault Detection of Inter-Turn Short-Circuited PMSM. *IEEE Trans. Instrum. Meas.* **2024**, *73*, 3523810. [CrossRef]
20. Williamson, S.; Mirzoian, K. Analysis of Cage Induction Motors with Stator Winding Faults. *IEEE Trans. Power Appar. Syst.* **1985**, *PAS-104*, 1838–1842. [CrossRef]
21. Jeong, H.; Moon, S.; Kim, S.W. An Early Stage Interturn Fault Diagnosis of PMSMs by Using Negative-Sequence Components. *IEEE Trans. Ind. Electron.* **2017**, *64*, 5701–5708. [CrossRef]
22. Dorrell, D.G.; Makhoba, K. Detection of Inter-Turn Stator Faults in Induction Motors Using Short-Term Averaging of Forward and Backward Rotating Stator Current Phasors for Fast Prognostics. *IEEE Trans. Magn.* **2017**, *53*, 1700107. [CrossRef]
23. Ge, Y.; Song, B.; Pei, Y.; Mollet, Y.A.B.; Gyselinck, J.J.C. Analytical Expressions of Isolation Indicators for Permanent-Magnet Synchronous Machines under Stator Short-Circuit Faults. *IEEE Trans. Energy Convers.* **2019**, *34*, 984–992. [CrossRef]
24. Bahloul, I.; Bouzid, M.B.K.; Khil, S.K.E.; Champenois, G. Robust Novel Indicator to Distinguish between an Inter-Turn Short Circuit Fault and Load Unbalance in PMSG. *IEEE Trans. Ind. Appl.* **2023**, *59*, 3200–3209. [CrossRef]
25. Laadjal, K.; Bento, F.; Henriques, K.; Marques Cardoso, A.J.; Sahraoui, M. A Novel Indicator-Based on-Line Diagnostics Technique of Inter-Turn Short-Circuit Faults in Synchronous Reluctance Machines. *IEEE J. Emerg. Sel. Top. Power Electron.* **2023**, *11*, 3492–3501. [CrossRef]
26. Naderi, P.; Fathi, A. Fault Diagnosis/Separation of Surface Mounted Permanent Magnet Synchronous Machine by Current and Its Homopolar Orders Analysis. *IEEE Trans. Energy Convers.* **2022**, *38*, 1246–1256. [CrossRef]
27. Park, J.-K.; Hur, J. Detection of Inter-Turn and Dynamic Eccentricity Faults Using Stator Current Frequency Pattern in IPM-Type BLDC Motors. *IEEE Trans. Ind. Electron.* **2016**, *63*, 1771–1780. [CrossRef]
28. Lee, S.-T.; Hur, J. Detection Technique for Stator Inter-Turn Faults in BLDC Motors Based on Third-Harmonic Components of Line Currents. *IEEE Trans. Ind. Appl.* **2017**, *53*, 143–150. [CrossRef]
29. Wang, B.; Wang, J.; Griffo, A.; Sen, B. Stator Turn Fault Detection by Second Harmonic in Instantaneous Power for a Triple-Redundant Fault-Tolerant PM Drive. *IEEE Trans. Ind. Electron.* **2018**, *65*, 7279–7289. [CrossRef]
30. Duan, R.; Wu, L.; Lyu, Z.; Zhan, H.; Song, P. Harmonic Subspace Signature-Based Detection and Localization of Inter-Turn Short Circuit Fault for Dual Three-Phase PMSM with VSD Scheme. *IEEE Trans. Transp. Electrif.* **2024**, *10*, 9652–9664. [CrossRef]
31. Huang, S.; Aggarwal, A.; Strangas, E.G.; Li, K.; Niu, F.; Huang, X. Robust Stator Winding Fault Detection in PMSMs with Respect to Current Controller Bandwidth. *IEEE Trans. Power Electron.* **2021**, *36*, 5032–5042. [CrossRef]
32. Rosero, J.A.; Romeral, L.; Ortega, J.A.; Rosero, E. Short-Circuit Detection by Means of Empirical Mode Decomposition and Wigner–Ville Distribution for PMSM Running under Dynamic Condition. *IEEE Trans. Ind. Electron.* **2009**, *56*, 4534–4547. [CrossRef]
33. Dogan, Z.; Tetik, K. Diagnosis of Inter-Turn Faults Based on Fault Harmonic Component Tracking in LSPMSMs Working under Nonstationary Conditions. *IEEE Access* **2021**, *9*, 92101–92112. [CrossRef]
34. Chen, C.-S.; Lin, C.-J.; Yang, F.-J.; Lin, F.-C. Model Design of Inter-Turn Short Circuits in Internal Permanent Magnet Synchronous Motors and Application of Wavelet Transform for Fault Diagnosis. *Appl. Sci.* **2024**, *14*, 9570. [CrossRef]
35. Boileau, T.; Leboeuf, N.; Nahid-Mobarakeh, B.; Meibody-Tabar, F. Synchronous Demodulation of Control Voltages for Stator Interturn Fault Detection in PMSM. *IEEE Trans. Power Electron.* **2013**, *28*, 5647–5654. [CrossRef]
36. Bellini, A.; Filippetti, F.; Franceschini, G.; Tassoni, C. Closed-Loop Control Impact on the Diagnosis of Induction Motors Faults. *IEEE Trans. Ind. Appl.* **2000**, *36*, 1318–1329. [CrossRef]

37. Wei, D.; Liu, K.; Hu, W.; Peng, X.; Chen, Y.; Ding, R. Short-Time Adaline Based Fault Feature Extraction for Inter-Turn Short Circuit Diagnosis of PMSM via Residual Insulation Monitoring. *IEEE Trans. Ind. Electron.* **2023**, *70*, 3103–3114. [CrossRef]
38. Wei, D.; Liu, K.; Huang, J.; Wang, J.; Zhou, S.; Cai, H.; Chen, J. Instantaneous Phase Estimation Based Single-Signal Diagnosis for Inter-Turn Short Circuit Fault in PMSMs. *IEEE Trans. Energy Convers.* **2024**, *[Online early access]*. [CrossRef]
39. Ghods, M.; Tabarniarami, Z.; Faiz, J.; Bazrafshan, M.A. Turn-to-Turn and Phase-to-Phase Short Circuit Fault Detection of Wind Turbine Permanent Magnet Generator Based on Equivalent Magnetic Network Modelling by Wavelet Transform Approach. *IET Electr. Power Appl.* **2024**, *18*, 1005–1020. [CrossRef]
40. Niu, F.; Xu, M.; Zhou, F.; Huang, S.; Xu, Z.; Zhang, L.; Aggarwal, A. Accurate Interturn Short-Circuit Faults Diagnosis in PMSMs under Variable Operating Conditions by Signal Compensation. *IEEE Trans. Power Electron.* **2024**, *40*, 3530–3542. [CrossRef]
41. Fonseca, D.S.B.; Santos, C.M.C.; Cardoso, A.J.M. Stator Faults Modeling and Diagnostics of Line-Start Permanent Magnet Synchronous Motors. *IEEE Trans. Ind. Appl.* **2020**, *56*, 2590–2599. [CrossRef]
42. Qiao, J.; Yin, X.; Wang, Y.; Lu, Q.; Tan, L.; Zhu, L. A Stator Internal Short-Circuit Fault Protection Method for Turbo-Generator Based on Instantaneous Power Oscillation Ratio. *IEEE Trans. Energy Convers.* **2023**, *38*, 1903–1912. [CrossRef]
43. Haddad, R.Z.; Lopez, C.A.; Foster, S.N.; Strangas, E.G. A Voltage-Based Approach for Fault Detection and Separation in Permanent Magnet Synchronous Machines. *IEEE Trans. Ind. Appl.* **2017**, *53*, 5305–5314. [CrossRef]
44. Moon, S.; Jeong, H.; Lee, H.; Kim, S.W. Detection and Classification of Demagnetization and Interturn Short Faults of IPMSMs. *IEEE Trans. Ind. Electron.* **2017**, *64*, 9433–9441. [CrossRef]
45. Ullah, Z.; Lee, S.-T.; Hur, J. A Torque Angle-Based Fault Detection and Identification Technique for IPMSM. *IEEE Trans. Ind. Appl.* **2020**, *56*, 170–182. [CrossRef]
46. Tabarniarami, Z.; Ghods, M.; Faiz, J.; Abedini, M. Online Diagnosis of Short Circuit Faults of Permanent Magnet Synchronous Generator by Short-Time Analysis of the Three Phase Amplitude-Phase Signal Based on Analytical Modeling. *IEEE Trans. Transp. Electrif.* **2024**, *10*, 10029–10042. [CrossRef]
47. Hang, J.; Wang, X.; Li, W.; Ding, S. Interturn Short-Circuit Fault Diagnosis and Fault-Tolerant Control of DTP-PMSM Based on Subspace Current Residuals. *IEEE Trans. Power Electron.* **2024**, *40*, 3395–3404. [CrossRef]
48. Wang, H.; Hu, J.; Li, Y. Fault Phase Location for Interturn Short Circuit Faults in Symmetrical Six-Phase PMSMs Based on Subspace Current Residual. *IEEE Trans. Transp. Electrif.* **2024**, *10*, 8336–8345. [CrossRef]
49. Hu, J.; Wang, H.; Li, Y. Model-Based Severity Monitoring for Interturn Short Circuit Faults in Symmetrical Six-Phase PMSMs Using Subspace Current Residuals. *IEEE Trans. Power Electron.* **2023**, *38*, 16142–16152. [CrossRef]
50. Sen, B.; Wang, J. Stator Interturn Fault Detection in Permanent-Magnet Machines Using PWM Ripple Current Measurement. *IEEE Trans. Ind. Electron.* **2016**, *63*, 3148–3157. [CrossRef]
51. Wang, B.; Hu, J.; Wang, G.; Hua, W. A Novel Stator Turn Fault Detection Technique by Using Equivalent High Frequency Impedance. *IEEE Access* **2020**, *8*, 130540–130550. [CrossRef]
52. Hu, R.; Wang, J.; Sen, B.; Mills, A.R.; Chong, E.; Sun, Z. PWM Ripple Currents Based Turn Fault Detection for Multiphase Permanent Magnet Machines. *IEEE Trans. Ind. Appl.* **2017**, *53*, 2740–2751. [CrossRef]
53. Hu, R.; Wang, J.; Mills, A.; Chong, E.; Sun, Z. Detection and Classification of Turn Fault and High-resistance Connection Fault in Inverter-fed Permanent Magnet Machines Based on High-frequency Signals. *J. Eng.* **2019**, *2019*, 4278–4282. [CrossRef]
54. Hu, R.; Wang, J.; Mills, A.R.; Chong, E.; Sun, Z. Detection and Classification of Turn Fault and High Resistance Connection Fault in Permanent Magnet Machines Based on Zero Sequence Voltage. *IEEE Trans. Power Electron.* **2020**, *35*, 1922–1933. [CrossRef]
55. Gao, F.; Zhang, G.; Li, M.; Gao, Y.; Zhuang, S. Inter-Turn Fault Identification of Surface-Mounted Permanent Magnet Synchronous Motor Based on Inverter Harmonics. *Energies* **2020**, *13*, 899. [CrossRef]
56. Wang, B.; Luo, L.; Fu, W.; Hua, W.; Wang, G.; Wang, Z. Study on the PWM Ripple Current Based Turn Fault Detection for Interior PM Machine. *IEEE Trans. Transp. Electrif.* **2021**, *7*, 1537–1547. [CrossRef]
57. Zhang, J.; Xu, Z.; Wang, J.; Zhao, J.; Din, Z.; Cheng, M. Detection and Discrimination of Incipient Stator Faults for Inverter-Fed Permanent Magnet Synchronous Machines. *IEEE Trans. Ind. Electron.* **2021**, *68*, 7505–7515. [CrossRef]
58. Xu, Z.; Zhang, J.; Zhang, Y.; Zhao, J. Winding Condition Monitoring for Inverter-Fed PMSM Using High-Frequency Current Injection. *IEEE Trans. Ind. Appl.* **2021**, *57*, 5818–5828. [CrossRef]
59. Hu, R.; Wang, J.; Mills, A.R.; Chong, E.; Sun, Z. High-Frequency Voltage Injection Based Stator Interturn Fault Detection in Permanent Magnet Machines. *IEEE Trans. Power Electron.* **2021**, *36*, 785–794. [CrossRef]
60. Wang, H.; Wu, Z.; Zhou, F.; Cao, W.; Hu, C.; Lu, S. Diagnosis of Interturn Short Circuit Fault in BLDCM Based on Coupled High-Frequency Signal Injection. *IEEE Trans. Instrum. Meas.* **2024**, *73*, 3532310. [CrossRef]
61. Xu, Z.; Zhang, J.; Cheng, M. Investigation of Signal Injection Methods for Fault Detection of PMSM Drives. *IEEE Trans. Energy Convers.* **2022**, *37*, 2207–2216. [CrossRef]
62. Xu, Z.; Zhang, J.; Xiong, J.; Wu, Y.; Cheng, M. An Improved High Frequency Voltage Injection Method for Inter-Turn Short-Circuit Fault Detection in PMSMs. *IEEE Trans. Transp. Electrif.* **2022**, *9*, 3228–3239. [CrossRef]

63. Fang, X.; Gao, J.; Lu, J.; Zhang, J.; Li, H. Early Fault Detection of Stator Inter-Turn Short Circuit of Asynchronous Motor Based on Rotating High Frequency Voltage Injection. *IEEE Trans. Transp. Electrif.* 2024; *Online early access*. [CrossRef]
64. Qi, Y.; Zafarani, M.; Akin, B.; Fedigan, S.E. Analysis and Detection of Inter-Turn Short-Circuit Fault through Extended Self-Commissioning. *IEEE Trans. Ind. Appl.* **2017**, *53*, 2730–2739. [CrossRef]
65. Baruti, K.H.; Gurusamy, V.; Erturk, F.; Akin, B. A Robust and Practical Approach to Estimate the Number of Shorted Turns in PMSM with ITSC Faults. *IEEE J. Emerg. Sel. Top. Power Electron.* **2021**, *9*, 2839–2849. [CrossRef]
66. Hang, J.; Ding, S.; Zhang, J.; Cheng, M.; Chen, W.; Wang, Q. Detection of Interturn Short-Circuit Fault for PMSM with Simple Fault Indicator. *IEEE Trans. Energy Convers.* **2016**, *31*, 1697–1699. [CrossRef]
67. Haje Obeid, N.; Battiston, A.; Boileau, T.; Nahid-Mobarakeh, B. Early Intermittent Interturn Fault Detection and Localization for a Permanent Magnet Synchronous Motor of Electrical Vehicles Using Wavelet Transform. *IEEE Trans. Transp. Electrif.* **2017**, *3*, 694–702. [CrossRef]
68. Hang, J.; Zhang, J.; Xia, M.; Ding, S.; Hua, W. Interturn Fault Diagnosis for Model-Predictive-Controlled-PMSM Based on Cost Function and Wavelet Transform. *IEEE Trans. Power Electron.* **2020**, *35*, 6405–6418. [CrossRef]
69. Ray, D.K.; Roy, T.; Chattopadhyay, S. Skewness Scanning for Diagnosis of a Small Inter-Turn Fault in Quadcopter's Motor Based on Motor Current Signature Analysis. *IEEE Sens. J.* **2021**, *21*, 6952–6961. [CrossRef]
70. Park, C.H.; Lee, J.; Kim, H.; Suh, C.; Youn, M.; Shin, Y.; Ahn, S.-H.; Youn, B.D. Drive-Tolerant Current Residual Variance (DTCRV) for Fault Detection of a Permanent Magnet Synchronous Motor under Operational Speed and Load Torque Conditions. *IEEE Access* **2021**, *9*, 49055–49068. [CrossRef]
71. Jafari, A.; Faiz, J.; Jarrahi, M.A. A Simple and Efficient Current-Based Method for Interturn Fault Detection in BLDC Motors. *IEEE Trans. Ind. Inform.* **2021**, *17*, 2707–2715. [CrossRef]
72. Da, Y.; Shi, X.; Krishnamurthy, M. A New Approach to Fault Diagnostics for Permanent Magnet Synchronous Machines Using Electromagnetic Signature Analysis. *IEEE Trans. Power Electron.* **2013**, *28*, 4104–4112. [CrossRef]
73. Huang, W.; Du, B.; Li, T.; Sun, Y.; Cheng, Y.; Cui, S. Interturn Short-Circuit Fault Diagnosis of Interior Permanent Magnet Synchronous Motor for Electric Vehicle Based on Search Coil. *IEEE Trans. Power Electron.* **2023**, *38*, 2506–2515. [CrossRef]
74. Gao, C.; Miao, Z.; Sang, X.; Xu, X.; Si, J.; Alkahtani, M. A Multi-Faults Online Detection and Identification Method for Concentrated Winding PMSM Using Search Coil Array. *IEEE Trans. Transp. Electrif.* **2024**, *Online early access*. [CrossRef]
75. Mühlthaler, J.; Lehner, B.; Reeh, A. Detection of Inter-Turn Short-Circuits in Permanent Magnet Machines Based on Rogowski & Search Coil Based Monitoring. In Proceedings of the 2024 International Conference on Electrical Machines (ICEM), Torino, Italy, 1–4 September 2024; IEEE: Piscataway, NJ, USA, 2024; pp. 1–8.
76. Zeng, C.; Huang, S.; Yang, Y.; Wu, D. Inter-turn Fault Diagnosis of Permanent Magnet Synchronous Machine Based on Tooth Magnetic Flux Analysis. *IET Electr. Power Appl.* **2018**, *12*, 837–844. [CrossRef]
77. Li, R.; Fang, H.; Li, D.; Qu, R.; Yang, S.; Wang, R. A Search Coil Design Method of PMSM for Detection of Inter-Turn Short-Circuit Fault. *IEEE Trans. Ind. Electron.* **2023**, *71*, 3964–3974. [CrossRef]
78. Liu, X.; Miao, W.; Xu, Q.; Cao, L.; Liu, C.; Pong, P.W.T. Inter-Turn Short-Circuit Fault Detection Approach for Permanent Magnet Synchronous Machines through Stray Magnetic Field Sensing. *IEEE Sens. J.* **2019**, *19*, 7884–7895. [CrossRef]
79. Irhoumah, M.; Pusca, R.; Lefevre, E.; Mercier, D.; Romary, R. Detection of the Stator Winding Inter-Turn Faults in Asynchronous and Synchronous Machines through the Correlation between Harmonics of the Voltage of Two Magnetic Flux Sensors. *IEEE Trans. Ind. Appl.* **2019**, *55*, 2682–2689. [CrossRef]
80. Gurusamy, V.; Bostanci, E.; Li, C.; Qi, Y.; Akin, B. A Stray Magnetic Flux-Based Robust Diagnosis Method for Detection and Location of Interturn Short Circuit Fault in PMSM. *IEEE Trans. Instrum. Meas.* **2021**, *70*, 3500811. [CrossRef]
81. Eldeeb, H.H.; Berzoy, A.; Mohammed, O. Stator Fault Detection on DTC-Driven IM via Magnetic Signatures Aided by 2-D FEA Co-Simulation. *IEEE Trans. Magn.* **2019**, *55*, 8101505. [CrossRef]
82. Assaf, T.; Henao, H.; Capolino, G.A. Simplified Axial Flux Spectrum Method to Detect Incipient Stator Inter-Turn Short-Circuits in Induction Machine. In Proceedings of the 2004 IEEE International Symposium on Industrial Electronics, Ajaccio, France, 4–7 May 2004; Volume 2, pp. 815–819.
83. Lamim Filho, P.C.M.; Rabelo Baccarini, L.M.; Batista, F.B.; Araujo, A.C. Orbit Analysis from a Stray Flux Full Spectrum for Induction Machine Fault Detection. *IEEE Sens. J.* **2021**, *21*, 16152–16161. [CrossRef]
84. Kumar, P.S.; Xie, L.; Halick, M.S.M.; Vaiyapuri, V. Stator End-Winding Thermal and Magnetic Sensor Arrays for Online Stator Inter-Turn Fault Detection. *IEEE Sens. J.* **2021**, *21*, 5312–5321. [CrossRef]
85. Bai, W.; Zhou, X.; Wang, Y.; Zeng, Q.; Zhan, S.; Hua, X.; Bao, G. Vibration Analysis of the Electric Drive System with Inter-Turn Short-Circuit and Gear Spalling Faults. *J. Vib. Eng. Technol.* **2023**, *11*, 3595–3605. [CrossRef]
86. Wu, Y.-H.; Liu, M.-Y.; Song, H.; Li, C.; Yang, X.-L. A Temperature and Magnetic Field-Based Approach for Stator Inter-Turn Fault Detection. *IEEE Sens. J.* **2022**, *22*, 17799–17807. [CrossRef]
87. Wei, D.; Liu, K.; Zhu, Z.-Q.; Zhou, S.; Wang, J.; Chen, Y. Rotor Speed Signature Analysis-Based Inter-Turn Short Circuit Fault Detection for Permanent Magnet Synchronous Machines. *IET Electr. Power Appl.* **2024**, *18*, 1187–1199. [CrossRef]

88. Wei, D.; Liu, K.; Wang, J.; Zhou, S.; Cai, H.; Chen, J. Detection of Inter-Turn Short Circuit Fault in Permanent Magnet Synchronous Machine under Phase Current Reconstruction Control. In Proceedings of the 2023 26th International Conference on Electrical Machines and Systems (ICEMS), Zhuhai, China, 5–8 November 2023; IEEE: Piscataway, NJ, USA, 2023; pp. 2164–2168.
89. Liu, C.; Xiao, L.; Zou, J.; Xu, Y.; Li, S. Analysis and Monitoring Method for Inter-Turn Short-Circuit Fault for PMSM. *IEEE Trans. Magn.* **2023**, *59*, 8103106. [CrossRef]
90. Leboeuf, N.; Boileau, T.; Nahid-Mobarakeh, B.; Clerc, G.; Meibody-Tabar, F. Real-Time Detection of Interturn Faults in PM Drives Using Back-EMF Estimation and Residual Analysis. *IEEE Trans. Ind. Appl.* **2011**, *47*, 2402–2412. [CrossRef]
91. Mazzoletti, M.A.; Bossio, G.R.; De Angelo, C.H.; Espinoza-Trejo, D.R. A Model-Based Strategy for Interturn Short-Circuit Fault Diagnosis in PMSM. *IEEE Trans. Ind. Electron.* **2017**, *64*, 7218–7228. [CrossRef]
92. Hu, R.; Wang, J.; Mills, A.R.; Chong, E.; Sun, Z. Current-Residual-Based Stator Interturn Fault Detection in Permanent Magnet Machines. *IEEE Trans. Ind. Electron.* **2021**, *68*, 59–69. [CrossRef]
93. Castro Palavicino, P.; Sarlioglu, B. Estimation of Position and Shorted Turns Percentage of an Inter-Turn Short Circuit in Interior Permanent Magnet Synchronous Machines Based on a Current Observer and Stationary Reference Frame Tracking. *IEEE Trans. Ind. Appl.* **2023**, *59*, 4066–4075. [CrossRef]
94. Mahmoudi, A.; Jlassi, I.; Cardoso, A.J.M.; Yahia, K.; Sahraoui, M. Inter-Turn Short-Circuit Faults Diagnosis in Synchronous Reluctance Machines, Using the Luenberger State Observer and Current's Second-Order Harmonic. *IEEE Trans. Ind. Electron.* **2022**, *69*, 8420–8429. [CrossRef]
95. Qin, Y.; Li, G.J.; Zhu, Z.Q.; Foster, M.P.; Stone, D.A.; Jia, C.J.; McKeever, P. Model-Based Luenberger State Observer for Detecting Interturn Short-Circuits in PM Machines. *IEEE Trans. Transp. Electrif.* **2024**, *Online early access*. [CrossRef]
96. Belkhadir, A.; Pusca, R.; Romary, R.; Belkhayat, D.; Zidani, Y. Detection of External Rotor PMSM Inter-Turn Short Circuit Fault Using Extended Kalman Filter. In Proceedings of the 2023 IEEE 14th International Symposium on Diagnostics for Electrical Machines, Power Electronics and Drives (SDEMPED), Chania, Greece, 28–31 August 2023; IEEE: Piscataway, NJ, USA, 2023; pp. 491–497.
97. Chen, Z.; Liang, D.; Jia, S.; Yang, L.; Yang, S. Incipient Interturn Short-Circuit Fault Diagnosis of Permanent Magnet Synchronous Motors Based on the Data-Driven Digital Twin Model. *IEEE J. Emerg. Sel. Top. Power Electron.* **2023**, *11*, 3514–3524. [CrossRef]
98. Hang, J.; Hu, Q.; Sun, W.; Ren, X.; Ding, S.; Huang, Y.; Hua, W. A Voltage-Distortion-Based Method for Robust Detection and Location of Interturn Fault in Permanent Magnet Synchronous Machine. *IEEE Trans. Power Electron.* **2022**, *37*, 11174–11186. [CrossRef]
99. Du, B.; Wu, S.; Han, S.; Cui, S. Interturn Fault Diagnosis Strategy for Interior Permanent-Magnet Synchronous Motor of Electric Vehicles Based on Digital Signal Processor. *IEEE Trans. Ind. Electron.* **2016**, *63*, 1694–1706. [CrossRef]
100. Chen, Q.; Han, X.; Liu, G.; Zhao, W.; Shi, H. Inter-Turn Fault Diagnosis and Control for Five-Phase PMSMs by Disturbance Observer. *IEEE Trans. Ind. Electron.* **2024**, *71*, 13901–13909. [CrossRef]
101. Cui, R.; Fan, Y.; Li, C. On-Line Inter-Turn Short-Circuit Fault Diagnosis and Torque Ripple Minimization Control Strategy Based on OW Five-Phase BFTHE-IPM. *IEEE Trans. Energy Convers.* **2018**, *33*, 2200–2209. [CrossRef]
102. Xu, Y.; Wang, Y.; Zou, J. An Inter-Turn Short-Circuits Fault Detection Strategy Considering Inverter Nonlinearity and Current Measurement Errors for Sensorless Control of SPMSM. *IEEE Trans. Ind. Electron.* **2022**, *69*, 11709–11722. [CrossRef]
103. Upadhyay, A.; Alakula, M. A Theoretical Study of Stator Flux Linkage DC Offset Based Stator Fault Detection for PMSM Drive Systems. In Proceedings of the 2022 IEEE Vehicle Power and Propulsion Conference (VPPC), Merced, CA, USA, 1–4 November 2022; pp. 1–6.
104. Yang, Y.; Chen, Y.; Hao, W. Online Detection of Inter-turn Short-circuit Fault in Dual-redundancy Permanent Magnet Synchronous Motor. *IET Electr. Power Appl.* **2020**, *15*, 104–113. [CrossRef]
105. Feng, X.; Wang, B.; Liu, C.; Zeng, J.; Wang, Z. Research on Inter-Turn Short-Circuit Fault Diagnosis Method Based on High Frequency Voltage Residual for PMSM. *Trans. Electr. Mach. Syst.* **2023**, *7*, 256–265. [CrossRef]
106. Wang, H.; Hu, J.; Li, Y. Interturn Fault Severity Monitoring in Symmetrical Six-Phase PMSMs Using Subspace Negative-Sequence High-Frequency Current Residuals. *IEEE Trans. Power Electron.* **2024**, *39*, 3613–3622. [CrossRef]
107. Fan, P.; Zhang, Y. A Detection Method for Interturn Short-Circuit Fault of Five-Phase Surface Mounted PMSM. In Proceedings of the 2023 26th International Conference on Electrical Machines and Systems (ICEMS), Zhuhai, China, 5–8 November 2023; IEEE: Piscataway, NJ, USA, 2023; pp. 68–73.
108. Aubert, B.; Regnier, J.; Caux, S.; Alejo, D. Kalman-Filter-Based Indicator for Online Interturn Short Circuits Detection in Permanent-Magnet Synchronous Generators. *IEEE Trans. Ind. Electron.* **2015**, *62*, 1921–1930. [CrossRef]
109. El Sayed, W.; Abd El Geliel, M.; Lotfy, A. Fault Diagnosis of PMSG Stator Inter-Turn Fault Using Extended Kalman Filter and Unscented Kalman Filter. *Energies* **2020**, *13*, 2972. [CrossRef]
110. Zhang, J.; Zhan, W.; Ehsani, M. Diagnosis and Fault-Tolerant Control of Permanent Magnet Synchronous Motors with Interturn Short-Circuit Fault. *IEEE Trans. Control Syst. Technol.* **2023**, *31*, 1909–1916. [CrossRef]

111. Moseler, O.; Isermann, R. Model-Based Fault Detection for a Brushless DC Motor Using Parameter Estimation. In Proceedings of the IECON '98 24th Annual Conference of the IEEE Industrial Electronics Society (Cat. No.98CH36200), Aachen, Germany, 31 August–4 September 1998; IEEE: Piscataway, NJ, USA, 1998; Volume 4, pp. 1956–1960.
112. Moseler, O.; Isermann, R. Application of Model-Based Fault Detection to a Brushless DC Motor. *IEEE Trans. Ind. Electron.* **2000**, *47*, 1015–1020. [CrossRef]
113. Aswad, R.A.K.; Jassim, B.M.H. Detection and Localization of the Stator Winding Inter-Turn Fault in Induction Motors Based on Parameters Estimation Using Genetic Algorithm. *J. Inst. Eng. India Ser. B* **2022**, *103*, 405–414. [CrossRef]
114. Zezula, L.; Kozovsky, M.; Blaha, P. Diagnostics of Interturn Short Circuits in PMSMs with Online Fault Indicators Estimation. *IEEE Trans. Ind. Electron.* **2024**, *71*, 15001–15011. [CrossRef]
115. He, Q.; Pan, J.; Lyu, X. Early Performance Degradation Detecting Method for PMSM Based on Change in Frequency Domain Features of Three-Phase Stator Current. *IEEE Access* **2023**, *11*, 123361–123372. [CrossRef]
116. Kang, Y.; Yao, L. Fault Isolation and Estimation for Turn-to-Turn Short Circuit in Permanent Magnet Synchronous Motor. *IEEE Trans. Instrum. Meas.* **2024**, *73*, 3000811. [CrossRef]
117. Xu, Z.; Hu, C.; Yang, F.; Kuo, S.-H.; Goh, C.-K.; Gupta, A.; Nadarajan, S. Data-Driven Inter-Turn Short Circuit Fault Detection in Induction Machines. *IEEE Access* **2017**, *5*, 25055–25068. [CrossRef]
118. Wang, B.; Shen, C.; Xu, K.; Zheng, T. Turn-to-turn Short Circuit of Motor Stator Fault Diagnosis in Continuous State Based on Deep Auto-encoder. *IET Electr. Power Appl.* **2019**, *13*, 1598–1606. [CrossRef]
119. Mahmoud, M.S.; Huynh, V.K.; Senanyaka, J.S.L.; Robbersmyr, K.G. Robust Multiple-Fault Diagnosis of PMSM Drives Under Variant Operations and Noisy Conditions. *IEEE Open J. Ind. Electron. Soc.* **2023**, *4*, 762–772. [CrossRef]
120. Maraaba, L.S.; Milhem, A.S.; Nemer, I.A.; Al-Duwaish, H.; Abido, M.A. Convolutional Neural Network-Based Inter-Turn Fault Diagnosis in LSPMSMs. *IEEE Access* **2020**, *8*, 81960–81970. [CrossRef]
121. Shih, K.-J.; Hsieh, M.-F.; Chen, B.-J.; Huang, S.-F. Machine Learning for Inter-Turn Short-Circuit Fault Diagnosis in Permanent Magnet Synchronous Motors. *IEEE Trans. Magn.* **2022**, *58*, 8204307. [CrossRef]
122. Song, Q.; Wang, M.; Lai, W.; Zhao, S. On Bayesian Optimization-Based Residual CNN for Estimation of Inter-Turn Short Circuit Fault in PMSM. *IEEE Trans. Power Electron.* **2023**, *38*, 2456–2468. [CrossRef]
123. Wang, M.; Song, Q.; Lai, W. On Model-Based Transfer Learning Method for the Detection of Inter-Turn Short Circuit Faults in PMSM. *Sensors* **2023**, *23*, 9145. [CrossRef] [PubMed]
124. Li, Y.; Wang, R.; Mao, R.; Zhang, Y.; Zhu, K.; Li, Y.; Zhang, J. A Fault Diagnosis Method Based on an Improved Deep Q-Network for the Interturn Short Circuits of a Permanent Magnet Synchronous Motor. *IEEE Trans. Transp. Electrif.* **2024**, *10*, 3870–3887. [CrossRef]
125. Li, H.; Shen, J.; Shi, C.; Shi, T. Hybrid Learning Model-Based Inter-Turn Short Circuit Fault Diagnosis of PMSM. In Proceedings of the 2023 IEEE Transportation Electrification Conference and Expo, Asia-Pacific (ITEC Asia-Pacific), Chiang Mai, Thailand, 28 November–1 December 2023; IEEE: Piscataway, NJ, USA, 2023; pp. 1–6.
126. Parvin, F.; Faiz, J.; Qi, Y.; Kalhor, A.; Akin, B. A Comprehensive Inter-Turn Fault Severity Diagnosis Method for Permanent Magnet Synchronous Motors Based on Transformer Neural Networks. *IEEE Trans. Ind. Inform.* **2023**, *19*, 10923–10933. [CrossRef]
127. Lee, H.; Jeong, H.; Koo, G.; Ban, J.; Kim, S.W. Attention Recurrent Neural Network-Based Severity Estimation Method for Interturn Short-Circuit Fault in Permanent Magnet Synchronous Machines. *IEEE Trans. Ind. Electron.* **2021**, *68*, 3445–3453. [CrossRef]
128. Xue, B.; Zhang, M.; Browne, W.N. Particle Swarm Optimization for Feature Selection in Classification: A Multi-Objective Approach. *IEEE Trans. Cybern.* **2013**, *43*, 1656–1671. [CrossRef]
129. Grouz, F.; Sbita, L.; Boussak, M. Particle Swarm Optimization Based Fault Diagnosis for Non-Salient PMSM with Multi-Phase Inter-Turn Short Circuit. In Proceedings of the 2012 2nd International Conference on Communications, Computing and Control Applications CCCA'12, Marseilles, France, 6–8 December 2012; IEEE: Piscataway, NJ, USA, 2012; pp. 1–6.
130. Tomczyk, M.; Mielnik, R.; Plichta, A.; Gołdasz, I.; Sułowicz, M. Application of Genetic Algorithm for Inter-Turn Short Circuit Detection in Stator Winding of Induction Motor. *Energies* **2021**, *14*, 8523. [CrossRef]
131. Chen, X.; Qin, P.; Chen, Y.; Zhao, J.; Li, W.; Mao, Y.; Zhao, T. Inter-Turn Short Circuit Fault Diagnosis of PMSM. *Electronics* **2022**, *11*, 1576. [CrossRef]
132. Goode, P.V.; Chow, M.-Y. Using a Neural/Fuzzy System to Extract Heuristic Knowledge of Incipient Faults in Induction Motors. Part I-Methodology. *IEEE Trans. Ind. Electron.* **1995**, *42*, 131–138. [CrossRef]
133. Benbouzid, M.E.H.; Nejjari, H. A Simple Fuzzy Logic Approach for Induction Motors Stator Condition Monitoring. In Proceedings of the IEMDC 2001 IEEE International Electric Machines and Drives Conference (Cat. No.01EX485), Cambridge, MA, USA, 17–20 June 2001; IEEE: Piscataway, NJ, USA, 2001; pp. 634–639.
134. Yan, H.; Xu, Y.; Cai, F.; Zhang, H.; Zhao, W.; Gerada, C. PWM-VSI Fault Diagnosis for a PMSM Drive Based on the Fuzzy Logic Approach. *IEEE Trans. Power Electron.* **2019**, *34*, 759–768. [CrossRef]

135. Ballal, M.S.; Khan, Z.J.; Suryawanshi, H.M.; Sonolikar, R.L. Adaptive Neural Fuzzy Inference System for the Detection of Inter-Turn Insulation and Bearing Wear Faults in Induction Motor. *IEEE Trans. Ind. Electron.* **2007**, *54*, 250–258. [CrossRef]
136. Tallam, R.M.; Habetler, T.G.; Harley, R.G. Stator Winding Turn-Fault Detection for Closed-Loop Induction Motor Drives. *IEEE Trans. Ind. Appl.* **2003**, *39*, 720–724. [CrossRef]
137. Pietrzak, P.; Wolkiewicz, M. On-Line Detection and Classification of PMSM Stator Winding Faults Based on Stator Current Symmetrical Components Analysis and the KNN Algorithm. *Electronics* **2021**, *10*, 1786. [CrossRef]
138. Zhang, J.; Wang, Y.; Zhu, K.; Zhang, Y.; Li, Y. Diagnosis of Interturn Short-Circuit Faults in Permanent Magnet Synchronous Motors Based on Few-Shot Learning under a Federated Learning Framework. *IEEE Trans. Ind. Inform.* **2021**, *17*, 8495–8504. [CrossRef]
139. Haddad, R.Z.; Strangas, E.G. On the Accuracy of Fault Detection and Separation in Permanent Magnet Synchronous Machines Using MCSA/MVSA and LDA. *IEEE Trans. Energy Convers.* **2016**, *31*, 924–934. [CrossRef]
140. Maraaba, L.S.; Al-Hamouz, Z.M.; Milhem, A.S.; Abido, M.A. Neural Network-Based Diagnostic Tool for Detecting Stator Inter-Turn Faults in Line Start Permanent Magnet Synchronous Motors. *IEEE Access* **2019**, *7*, 89014–89025. [CrossRef]
141. Wei, D.; Liu, K.; Wang, J.; Zhou, S.; Li, K. ResNet-18 Based Inter-Turn Short Circuit Fault Diagnosis of PMSMs with Consideration of Speed and Current Loop Bandwidths. *IEEE Trans. Transp. Electrif.* **2023**, *10*, 5805–5818. [CrossRef]
142. Pietrzak, P.; Wolkiewicz, M.; Orlowska-Kowalska, T. PMSM Stator Winding Fault Detection and Classification Based on Bispectrum Analysis and Convolutional Neural Network. *IEEE Trans. Ind. Electron.* **2023**, *70*, 5192–5202. [CrossRef]
143. Li, L.; Liao, S.; Zou, B.; Liu, J. Mechanism-Based Fault Diagnosis Deep Learning Method for Permanent Magnet Synchronous Motor. *Sensors* **2024**, *24*, 6349. [CrossRef]
144. Zsuga, Á.; Dineva, A. Data-Driven Onboard Inter-Turn Short Circuit Fault Diagnosis for Electric Vehicles by Using Real-Time Simulation Environment. *IEEE Access* **2023**, *11*, 145447–145466. [CrossRef]
145. Kumar, R.R.; Randazzo, V.; Cirrincione, G.; Cirrincione, M.; Pasero, E.; Tortella, A.; Andriollo, M. Induction Machine Stator Fault Tracking Using the Growing Curvilinear Component Analysis. *IEEE Access* **2021**, *9*, 2201–2212. [CrossRef]
146. Wu, X.; Geng, Y.; Li, M.; Wang, W.; Tu, M. Inter-Turn Short Circuit Diagnosis of Permanent Magnet Synchronous Motor Based on Siamese Convolutional Neural Network Under Small Fault Samples. *IEEE Sens. J.* **2024**, *24*, 26982–26993. [CrossRef]
147. Chen, Z.; Liang, D.; Jia, S.; Yang, S. Model-Based Data Normalization for Data-Driven PMSM Fault Diagnosis. *IEEE Trans. Power Electron.* **2024**, *39*, 11596–11612. [CrossRef]
148. Lv, K.; Wang, D.; Huang, W.; Hu, J. Research on Fault Indicator for Integrated Fault Diagnosis System of PMSM Based on Stator Tooth Flux. *IEEE J. Emerg. Sel. Top. Power Electron.* **2024**, *12*, 985–996. [CrossRef]
149. Rafiei, V.; Khoshlessan, M.; Caicedo-Narvaez, C.; Fahimi, B. Detection of Inter-Turn Short Circuit in Stator Windings of Electric Machines Using Magnetic Symmetry Index and Machine Learning Methods. *IEEE Trans. Energy Convers.* **2024**, *Online early access*. [CrossRef]
150. Cao, W.; Huang, R.; Wang, H.; Lu, S.; Hu, Y.; Hu, C.; Huang, X. Analysis of Inter-Turn Short-Circuit Faults in Brushless DC Motors Based on Magnetic Leakage Flux and Back Propagation Neural Network. *IEEE Trans. Energy Convers.* **2023**, *38*, 2273–2281. [CrossRef]
151. Li, H.; Shi, T. Diagnosis of Inter-Turn Short-Circuit Incipient Fault in Permanent Magnet Synchronous Motors Using Input Current on the Power Side. *IEEE Trans. Ind. Inform.* **2024**, *20*, 13741–13752. [CrossRef]
152. Ibrahim, R.; Zemouri, R.; Kedjar, B.; Merkhouf, A.; Tahan, A.; Al-Haddad, K.; Lafleur, F. Non-Invasive Detection of Rotor Inter-Turn Short Circuit of a Hydrogenerator Using AI-Based Variational Autoencoder. *IEEE Trans. Ind. Appl.* **2023**, *60*, 28–37. [CrossRef]
153. Du, Y.; Wu, L.; Zhan, H.; Fang, Y. Influence of Dimensional Parameters on Three-Phase Short Circuit and Demagnetization in Surface-Mounted PM Machines. *IEEE Trans. Energy Convers.* **2021**, *36*, 2514–2523. [CrossRef]
154. Li, G.J.; Ren, B.; Zhu, Z.Q.; Foster, M.P.; Stone, D.A. Demagnetization Withstand Capability Enhancement of Surface Mounted PM Machines Using Stator Modularity. *IEEE Trans. Ind. Appl.* **2018**, *54*, 1302–1311. [CrossRef]
155. Urresty, J.-C.; Riba, J.-R.; Romeral, L. A Back-Emf Based Method to Detect Magnet Failures in PMSMs. *IEEE Trans. Magn.* **2013**, *49*, 591–598. [CrossRef]
156. Urresty, J.-C.; Riba, J.-R.; Delgado, M.; Romeral, L. Detection of Demagnetization Faults in Surface-Mounted Permanent Magnet Synchronous Motors by Means of the Zero-Sequence Voltage Component. *IEEE Trans. Energy Convers.* **2012**, *27*, 42–51. [CrossRef]
157. Zhan, H.; Wu, L.; Lyu, Z.; Du, Y.; Fang, Y. Uneven Demagnetization Fault Diagnosis in Dual Three-Phase Permanent Magnet Machines Based on Electrical Signal Difference. *IEEE Trans. Transp. Electrif.* **2022**, *9*, 3026–3039. [CrossRef]
158. Zafarani, M.; Goktas, T.; Akin, B.; Fedigan, S.E. An Investigation of Motor Topology Impacts on Magnet Defect Fault Signatures. *IEEE Trans. Ind. Electron.* **2017**, *64*, 32–42. [CrossRef]
159. Rajagopalan, S.; le Roux, W.; Habetler, T.G.; Harley, R.G. Dynamic Eccentricity and Demagnetized Rotor Magnet Detection in Trapezoidal Flux (Brushless DC) Motors Operating under Different Load Conditions. *IEEE Trans. Power Electron.* **2007**, *22*, 2061–2069. [CrossRef]

160. Garcia-Calva, T.A.; Gyftakis, K.N.; Skarmoutsos, G.A.; Mueller, M.; Morinigo-Sotelo, D.; Romero-Troncoso, R.D.J. Advanced Signal Processing Techniques for Demagnetization Detection in PM Generators at Variable Speed. *IEEE Trans. Ind. Appl.* **2023**, *60*, 174–183. [CrossRef]
161. Ruiz, J.R.R.; Rosero, J.A.; Espinosa, A.G.; Romeral, L. Detection of Demagnetization Faults in Permanent-Magnet Synchronous Motors under Nonstationary Conditions. *IEEE Trans. Magn.* **2009**, *45*, 2961–2969. [CrossRef]
162. Prieto, M.D.; Espinosa, A.G.; Ruiz, J.R.R.; Urresty, J.C.; Ortega, J.A. Feature Extraction of Demagnetization Faults in Permanent-Magnet Synchronous Motors Based on Box-Counting Fractal Dimension. *IEEE Trans. Ind. Electron.* **2011**, *58*, 1594–1605. [CrossRef]
163. Wang, C.; Delgado Prieto, M.; Romeral, L.; Chen, Z.; Blaabjerg, F.; Liu, X. Detection of Partial Demagnetization Fault in PMSMs Operating under Nonstationary Conditions. *IEEE Trans. Magn.* **2016**, *52*, 8105804. [CrossRef]
164. Gyftakis, K.N.; Garcia-Calva, T.A.; Skarmoutsos, G.A.; Morinigo-Sotelo, D.; Mueller, M.; Romero-Troncoso, R.D.J. Demagnetization Monitoring and Identification in PM Generators with Concentrated Windings during Transient Conditions. *IEEE Trans. Ind. Appl.* **2022**, *59*, 1510–1518. [CrossRef]
165. Espinosa, A.G.; Rosero, J.A.; Cusido, J.; Romeral, L.; Ortega, J.A. Fault Detection by Means of Hilbert–Huang Transform of the Stator Current in a PMSM with Demagnetization. *IEEE Trans. Energy Convers.* **2010**, *25*, 312–318. [CrossRef]
166. Chen, Z.; Liang, Z.; Liang, D.; Jia, S. Partial Demagnetization Fault Analysis and Diagnosis for Fractional Slot Concentrated Winding PMSMs Based on DQ-Axis Components. *IEEE Trans. Energy Convers.* **2024**, *Online early access*. [CrossRef]
167. Goktas, T.; Zafarani, M.; Akin, B. Discernment of Broken Magnet and Static Eccentricity Faults in Permanent Magnet Synchronous Motors. *IEEE Trans. Energy Convers.* **2016**, *31*, 578–587. [CrossRef]
168. Zafarani, M.; Goktas, T.; Akin, B. A Comprehensive Analysis of Magnet Defect Faults in Permanent Magnet Synchronous Motors. *IEEE Trans. Ind. Appl.* **2015**, *52*, 1331–1339. [CrossRef]
169. Radwan-Pragłowska, N.; Wegiel, T. Diagnostics of Interior PM Machine Rotor Faults Based on EMF Harmonics. *Energies* **2024**, *17*, 2198. [CrossRef]
170. Rasid, S.A.; Gyftakis, K.N.; Mueller, M. Comparative Investigation of Three Diagnostic Methods Applied to Direct-Drive Permanent Magnet Machines Suffering from Demagnetization. *Energies* **2023**, *16*, 2767. [CrossRef]
171. Gritli, Y.; Rossi, C.; Rizzoli, G.; Mengoni, M.; Tani, A.; Casadei, D. Robust Online Magnet Demagnetization Diagnosis in Asymmetrical Six-Phase AC Permanent Magnet Motor Drives. *IEEE Access* **2023**, *11*, 50769–50780. [CrossRef]
172. Hong, J.; Park, S.; Hyun, D.; Kang, T.; Lee, S.B.; Kral, C.; Haumer, A. Detection and Classification of Rotor Demagnetization and Eccentricity Faults for PM Synchronous Motors. *IEEE Trans. Ind. Appl.* **2012**, *48*, 923–932. [CrossRef]
173. Jongman, H.; Doosoo, H.; Sang Bin, L.; Ji-Yoon, Y.; Kwang-Woon, L. Automated Monitoring of Magnet Quality for Permanent-Magnet Synchronous Motors at Standstill. *IEEE Trans. Ind. Appl.* **2010**, *46*, 1397–1405. [CrossRef]
174. Fernandez, D.; Reigosa, D.D.; Guerrero, J.M.; Zhu, Z.-Q.; Briz, F. Permanent-Magnet Magnetization State Estimation Using High-Frequency Signal Injection. *IEEE Trans. Ind. Appl.* **2016**, *52*, 2930–2940. [CrossRef]
175. Diaz Reigosa, D.; Fernandez, D.; Zhu, Z.-Q.; Briz, F. PMSM Magnetization State Estimation Based on Stator-Reflected PM Resistance Using High-Frequency Signal Injection. *IEEE Trans. Ind. Appl.* **2015**, *51*, 3800–3810. [CrossRef]
176. He, W.; Hang, J.; Ding, S.; Sun, L.; Hua, W. Robust Diagnosis of Partial Demagnetization Fault in PMSMs Using Radial Air-Gap Flux Density under Complex Working Conditions. *IEEE Trans. Ind. Electron.* **2024**, *71*, 12001–12010. [CrossRef]
177. Zeng, C.; Huang, S.; Lei, J.; Wan, Z.; Yang, Y. Online Rotor Fault Diagnosis of Permanent Magnet Synchronous Motors Based on Stator Tooth Flux. *IEEE Trans. Ind. Appl.* **2021**, *57*, 2366–2377. [CrossRef]
178. Orviz, M.; Laborda, D.F.; Reigosa, D.; Lee, H.-J.; Rafaq, M.S.; Lee, S.B.; Briz, F. Demagnetization Detection and Severity Assessment in PMSMs Using Search Coils Exploiting Machine's Symmetry. *IEEE Trans. Ind. Appl.* **2023**, *59*, 4021–4034. [CrossRef]
179. Im, J.-H.; Kang, J.-K.; Heo, J.-H.; Hur, J. Utilization of Multiple Planar Search Coils for Diagnosing Imbalance Irreversible Demagnetization Faults in PMSMs Along the Z-Axis. *IEEE Trans. Ind. Appl.* **2024**, *60*, 5988–5997. [CrossRef]
180. Huang, W.; Chen, J.; Su, W.; Liu, H.; Lv, K.; Hu, J. A Period Energy Method for Demagnetization Detection in Surface Permanent Magnet Motors with Search Coils. *Electronics* **2023**, *12*, 3514. [CrossRef]
181. Naderi, P. Magnetic-Equivalent-Circuit Approach for Inter-Turn and Demagnetisation Faults Analysis in Surface Mounted Permanent-Magnet Synchronous Machines Using Pole Specific Search-Coil Technique. *IET Electr. Power Appl.* **2018**, *12*, 916–928. [CrossRef]
182. Rafaq, M.S.; Lee, H.; Park, Y.; Lee, S.-B.; Orviz Zapico, M.; Fernandez, D.; Diaz-Reigosa, D.; Briz, F. Airgap Search Coil Based Identification of PM Synchronous Motor Defects. *IEEE Trans. Ind. Electron.* **2022**, *69*, 6551–6560. [CrossRef]
183. Skarmoutsos, G.A.; Gyftakis, K.N.; Mueller, M. Detecting Partial Demagnetization in AFPM Generators by Monitoring Speed and EMF Induced in a Supplemental Winding. *IEEE Trans. Ind. Inform.* **2022**, *18*, 3295–3305. [CrossRef]
184. Gao, C.; Li, B.; Chen, H.; Xu, Y.; Xu, X.; Si, J.; Hu, Y. A Less-Invasive Method for Accurately Diagnosing of Demagnetization Fault in PMSM Using Rotor Partition. *IEEE Trans. Transp. Electrif.* **2022**, *9*, 2356–2366. [CrossRef]

185. Chen, H.; Fang, C.; Dong, J.; Lu, S.; Pires, V.; Martins, J.; Aguirre, M.P. Diagnosis of Inter-Turn Short-Circuit of SRM Based on Ratio of Current Components. *IEEE Trans. Transp. Electrif.* **2022**, *9*, 3319–3327. [CrossRef]
186. Skarmoutsos, G.A.; Gyftakis, K.N.; Mueller, M.A. A New Approach to PM Machine Fault Diagnostics Using Two Magnetically-Coupled Search-Coils. In Proceedings of the 2022 International Conference on Electrical Machines (ICEM), Valencia, Spain, 5–8 September 2022; pp. 1616–1621.
187. Jeong, J.; Lee, H.; Orviz, M.; Lee, S.B.; Reigosa, D.; Briz, F. Detection of Trailing Edge PM Demagnetization in Surface PM Synchronous Motors. *IEEE Trans. Ind. Appl.* **2023**, *59*, 3390–3399. [CrossRef]
188. Goktas, T.; Arkan, M.; Mamis, M.S.; Akin, B. Broken Rotor Bar Fault Monitoring Based on Fluxgate Sensor Measurement of Leakage Flux. In Proceedings of the 2017 IEEE International Electric Machines and Drives Conference (IEMDC), Miami, FL, USA, 21–24 May 2017; IEEE: Piscataway, NJ, USA, 2017; pp. 1–6.
189. Goktas, T.; Zafarani, M.; Lee, K.W.; Akin, B.; Sculley, T. Comprehensive Analysis of Magnet Defect Fault Monitoring through Leakage Flux. *IEEE Trans. Magn.* **2017**, *53*, 8201010. [CrossRef]
190. Xu, Q.; Liu, X.; Miao, W.; Pong, P.W.T.; Liu, C. Online Detecting Magnet Defect Fault in PMSG with Magnetic Sensing. *IEEE Trans. Transp. Electrif.* **2021**, *7*, 2775–2786. [CrossRef]
191. Reigosa, D.; Fernandez, D.; Park, Y.; Diez, A.B.; Lee, S.B.; Briz, F. Detection of Demagnetization in Permanent Magnet Synchronous Machines Using Hall-Effect Sensors. *IEEE Trans. Ind. Appl.* **2018**, *54*, 3338–3349. [CrossRef]
192. Reigosa, D.; Fernandez, D.; Martinez, M.; Park, Y.; Lee, S.B.; Briz, F. Permanent Magnet Synchronous Machine Non-Uniform Demagnetization Detection Using Zero-Sequence Magnetic Field Density. *IEEE Trans. Ind. Appl.* **2019**, *55*, 3823–3833. [CrossRef]
193. Park, Y.; Yang, C.; Lee, S.B.; Lee, D.-M.; Fernandez, D.; Reigosa, D.; Briz, F. Online Detection and Classification of Rotor and Load Defects in PMSMs Based on Hall Sensor Measurements. *IEEE Trans. Ind. Appl.* **2019**, *55*, 3803–3812. [CrossRef]
194. Park, Y.; Fernandez, D.; Lee, S.B.; Hyun, D.; Jeong, M.; Kommuri, S.K.; Cho, C.; Diaz Reigosa, D.; Briz, F. Online Detection of Rotor Eccentricity and Demagnetization Faults in PMSMs Based on Hall-Effect Field Sensor Measurements. *IEEE Trans. Ind. Appl.* **2019**, *55*, 2499–2509. [CrossRef]
195. Ebrahimi, B.M.; Faiz, J. Demagnetization Fault Diagnosis in Surface Mounted Permanent Magnet Synchronous Motors. *IEEE Trans. Magn.* **2013**, *49*, 1185–1192. [CrossRef]
196. Yang, C.; Wang, Y.; Qiu, H.; Chen, S.; Lian, Z. Electromagnetic Vibration of High-Voltage Line-Start Permanent Magnet Synchronous Motor with Demagnetization Fault. *J. Electr. Eng. Technol.* **2024**, *19*, 4143–4158. [CrossRef]
197. Ai, Q.; Wei, H.; Li, T.; Dou, H.; Zhao, W.; Zhang, Y. Online Demagnetization Fault Recognition for Permanent Magnet Motors Based on the Hall-Effect Analog Sampling. *IEEE Trans. Power Electron.* **2023**, *38*, 3600–3611. [CrossRef]
198. De Bisschop, J.; Abdallh, A.; Sergeant, P.; Dupre, L. Identification of Demagnetization Faults in Axial Flux Permanent Magnet Synchronous Machines Using an Inverse Problem Coupled with an Analytical Model. *IEEE Trans. Magn.* **2014**, *50*, 8104804. [CrossRef]
199. De Bisschop, J.; Vansompel, H.; Sergeant, P.; Dupre, L. Demagnetization Fault Detection in Axial Flux PM Machines by Using Sensing Coils and an Analytical Model. *IEEE Trans. Magn.* **2017**, *53*, 8203404. [CrossRef]
200. le Roux, W.; Harley, R.G.; Habetler, T.G. Detecting Rotor Faults in Low Power Permanent Magnet Synchronous Machines. *IEEE Trans. Power Electron.* **2007**, *22*, 322–328. [CrossRef]
201. Moon, S.; Lee, J.; Jeong, H.; Kim, S.W. Demagnetization Fault Diagnosis of a PMSM Based on Structure Analysis of Motor Inductance. *IEEE Trans. Ind. Electron.* **2016**, *63*, 3795–3803. [CrossRef]
202. Zhu, M.; Hu, W.; Kar, N.C. Torque-Ripple-Based Interior Permanent-Magnet Synchronous Machine Rotor Demagnetization Fault Detection and Current Regulation. *IEEE Trans. Ind. Appl.* **2017**, *53*, 2795–2804. [CrossRef]
203. Liu, Z.; Huang, J.; Li, B. Diagnosing and Distinguishing Rotor Eccentricity from Partial Demagnetisation of Interior PMSM Based on Fluctuation of High-frequency d -axis Inductance and Rotor Flux. *IET Electr. Power Appl.* **2017**, *11*, 1265–1275. [CrossRef]
204. Han, Y.; Chen, S.; Gong, C.; Zhao, X.; Zhang, F.; Li, Y. Accurate SM Disturbance Observer-Based Demagnetization Fault Diagnosis with Parameter Mismatch Impacts Eliminated for IPM Motors. *IEEE Trans. Power Electron.* **2023**, *38*, 5706–5710. [CrossRef]
205. Yi, C.-P.; Lin, Y.-J.; Ho, P.-J.; Yang, S.-C. Magnet Fault Diagnosis for Permanent Magnet Synchronous Motor Based on Flux Estimation With PWM Voltage Measurement. *IEEE Trans. Ind. Electron.* **2024**, *72*, 2100–2110. [CrossRef]
206. Vancini, L.; Mengoni, M.; Rizzoli, G.; Zarri, L.; Tani, A. Local Demagnetization Detection in Six-Phase Permanent Magnet Synchronous Machines. *IEEE Trans. Ind. Electron.* **2024**, *71*, 5508–5518. [CrossRef]
207. Kim, K.-T.; Lee, Y.-S.; Hur, J. Transient Analysis of Irreversible Demagnetization of Permanent-Magnet Brushless DC Motor With Interturn Fault Under the Operating State. *IEEE Trans. Ind. Appl.* **2014**, *50*, 3357–3364. [CrossRef]
208. Seo, M.-K.; Lee, T.-Y.; Ko, Y.-Y.; Kim, Y.-J.; Jung, S.-Y. Irreversible Demagnetization Analysis with Respect to Winding Connection and Current Ripple in Brushless DC Motor. *IEEE Trans. Appl. Supercond.* **2018**, *28*, 5203604. [CrossRef]
209. Khan, M.S.; Okonkwo, U.V.; Usman, A.; Rajpurohit, B.S. Finite Element Modeling of Demagnetization Fault in Permanent Magnet Direct Current Motors. In Proceedings of the 2018 IEEE Power & Energy Society General Meeting (PESGM), Portland, OR, USA, 5–10 August 2018; IEEE: Piscataway, NJ, USA, 2018; pp. 1–5.

210. Li, S.; Li, Y.; Sarlioglu, B. Partial Irreversible Demagnetization Assessment of Flux-Switching Permanent Magnet Machine Using Ferrite Permanent Magnet Material. *IEEE Trans. Magn.* **2015**, *51*, 8106209. [CrossRef]
211. Kim, K.-C.; Kim, K.; Kim, H.J.; Lee, J. Demagnetization Analysis of Permanent Magnets According to Rotor Types of Interior Permanent Magnet Synchronous Motor. *IEEE Trans. Magn.* **2009**, *45*, 2799–2802. [CrossRef]
212. Skowron, M.; Orlowska-Kowalska, T.; Kowalski, C.T. Detection of Permanent Magnet Damage of PMSM Drive Based on Direct Analysis of the Stator Phase Currents Using Convolutional Neural Network. *IEEE Trans. Ind. Electron.* **2022**, *69*, 13665–13675. [CrossRef]
213. Skowron, M. Transfer Learning-Based Fault Detection System of Permanent Magnet Synchronous Motors. *IEEE Access* **2024**, *12*, 135372–135389. [CrossRef]
214. Minaz, M.R.; Akcan, E. An Effective Method for Detection of Demagnetization Fault in Axial Flux Coreless PMSG with Texture-Based Analysis. *IEEE Access* **2021**, *9*, 17438–17449. [CrossRef]
215. Zhou, S.; Ma, C.; Ji, Z.; Feng, Q.; Zhao, Y.; Wang, Y.; Shen, Z.; Wang, D. A New Data-Driven Diagnosis Method for Compound Fault of Mixed Eccentricity and Demagnetization in External Rotor Permanent Magnet Motors. *IEEE Trans. Ind. Inf.* **2024**, *20*, 11794–11805. [CrossRef]
216. Pietrzak, P.; Wolkiewicz, M. Demagnetization Fault Diagnosis of Permanent Magnet Synchronous Motors Based on Stator Current Signal Processing and Machine Learning Algorithms. *Sensors* **2023**, *23*, 1757. [CrossRef] [PubMed]
217. Koutrakos, K.; Mitronikas, E. Outlier Detection for Permanent Magnet Synchronous Motor (PMSM) Fault Detection and Severity Estimation. *Appl. Sci.* **2024**, *14*, 4318. [CrossRef]
218. Kumar, L.; Nadarajan, S.; Vaiyapuri, V.; Gupta, A.; Soong, B.-H.; Nguyen, H.D. Decoupling of Demagnetization Characteristics to Improve the Turn-to-Turn Fault Detection in PMSM Using Machine Learning Methods. In Proceedings of the IECON 2023 49th Annual Conference of the IEEE Industrial Electronics Society, Singapore, 16–19 October 2023; IEEE: Piscataway, NJ, USA, 2023; pp. 1–6.
219. Du, B.; Huang, W.; Cheng, Y.; Chen, J.; Tao, R.; Cui, S. Fault Diagnosis and Separation of PMSM Rotor Faults Using Search Coil Based on MVSA and Random Forests. *IEEE Trans. Ind. Electron.* **2024**, *71*, 15089–15099. [CrossRef]
220. Kang, J.-K.; Yoo, D.-W.; Hur, J. Application and Verification of Voltage Angle-Based Fault Diagnosis Method in Six-Phase IPMSM. *IEEE Trans. Ind. Appl.* **2023**, *60*, 426–438. [CrossRef]
221. Meiwei, Z.; Weili, L.; Haoyue, T. Demagnetization Fault Diagnosis of the Permanent Magnet Motor for Electric Vehicles Based on Temperature Characteristic Quantity. *IEEE Trans. Transp. Electrif.* **2023**, *9*, 759–770. [CrossRef]
222. Song, J.; Zhao, J.; Zhang, X.; Dong, F.; Zhao, J.; Xu, L.; Yao, Z. Accurate Demagnetization Faults Detection of Dual-Sided Permanent Magnet Linear Motor Using Enveloping and Time-Domain Energy Analysis. *IEEE Trans. Ind. Inform.* **2020**, *16*, 6334–6346. [CrossRef]
223. Song, J.; Zhao, J.; Dong, F.; Zhao, J.; Xu, L.; Yao, Z. A New Demagnetization Fault Recognition and Classification Method for DPMSLM. *IEEE Trans. Ind. Inform.* **2020**, *16*, 1559–1570. [CrossRef]
224. Song, J.; Liu, S.; Duan, Z.; Wu, X.; Ding, W.; Wang, X.; Lu, S. DPMSLM Demagnetization Fault Detection Based on Texture Feature Analysis of Grayscale Fusion Image. *IEEE Trans. Instrum. Meas.* **2023**, *72*, 3510512. [CrossRef]
225. Gao, C.; Gao, B.; Xu, X.; Si, J.; Hu, Y. Automatic Demagnetization Fault Location of Direct-Drive Permanent Magnet Synchronous Motor Using Knowledge Graph. *IEEE Trans. Instrum. Meas.* **2024**, *73*, 3502312. [CrossRef]
226. Huang, F.; Zhang, X.; Qin, G.; Xie, J.; Peng, J.; Huang, S.; Long, Z.; Tang, Y. Demagnetization Fault Diagnosis of Permanent Magnet Synchronous Motors Using Magnetic Leakage Signals. *IEEE Trans. Ind. Inform.* **2022**, *19*, 6105–6116. [CrossRef]
227. Attestog, S.; Senanayaka, J.S.L.; Khang, H.V.; Robbersmyr, K.G. Robust Active Learning Multiple Fault Diagnosis of PMSM Drives with Sensorless Control under Dynamic Operations and Imbalanced Datasets. *IEEE Trans. Ind. Inform.* **2022**, *19*, 9291–9301. [CrossRef]
228. Zhu, Z.Q.; Wu, L.J.; Mohd Jamil, M.L. Distortion of Back-EMF and Torque of PM Brushless Machines Due to Eccentricity. *IEEE Trans. Magn.* **2013**, *49*, 4927–4936. [CrossRef]
229. Dorrell, D.G.; Hsieh, M.-F.; Guo, Y. Unbalanced Magnet Pull in Large Brushless Rare-Earth Permanent Magnet Motors With Rotor Eccentricity. *IEEE Trans. Magn.* **2009**, *45*, 4586–4589. [CrossRef]
230. Wei, Q.; Zeng, D.; Sun, Z.; Qiu, W.; Shuai, Z.; Li, W. An Improved Conformal Mapping Method for Electromagnetic Vibration Analysis in PMSMs With Rotor Eccentricity. *IEEE Trans. Appl. Supercond.* **2024**, *34*, 5204305. [CrossRef]
231. Zhu, Z.Q.; Wu, L.J.; Mohd Jamil, M.L. Influence of Pole and Slot Number Combinations on Cogging Torque in Permanent-Magnet Machines with Static and Rotating Eccentricities. *IEEE Trans. Ind. Appl.* **2014**, *50*, 3265–3277. [CrossRef]
232. Ebrahimi, B.M.; Faiz, J.; Roshtkhari, M.J. Static-, Dynamic-, and Mixed-Eccentricity Fault Diagnoses in Permanent-Magnet Synchronous Motors. *IEEE Trans. Ind. Electron.* **2009**, *56*, 4727–4739. [CrossRef]
233. Rajagopalan, S.; Aller, J.M.; Restrepo, J.A.; Habetler, T.G.; Harley, R.G. Analytic-Wavelet-Ridge-Based Detection of Dynamic Eccentricity in Brushless Direct Current (BLDC) Motors Functioning under Dynamic Operating Conditions. *IEEE Trans. Ind. Electron.* **2007**, *54*, 1410–1419. [CrossRef]

234. Rajagopalan, S.; Restrepo, J.A.; Aller, J.M.; Habetler, T.G.; Harley, R.G. Nonstationary Motor Fault Detection Using Recent Quadratic Time–Frequency Representations. *IEEE Trans. Ind. Appl.* **2008**, *44*, 735–744. [CrossRef]
235. Koura, M.B.; Boudinar, A.H.; Aimer, A.F.; Bendiabdellah, A.; Gherabi, Z. Diagnosis and Discernment between Eccentricity and Demagnetization Faults in PMSM Drives. *J. Power Electron.* **2021**, *21*, 563–573. [CrossRef]
236. Ebrahimi, B.M.; Faiz, J. Configuration Impacts on Eccentricity Fault Detection in Permanent Magnet Synchronous Motors. *IEEE Trans. Magn.* **2012**, *48*, 903–906. [CrossRef]
237. Jin, X.; Qiao, W.; Peng, Y.; Cheng, F.; Qu, L. Quantitative Evaluation of Wind Turbine Faults Under Variable Operational Conditions. *IEEE Trans. Ind. Appl.* **2016**, *52*, 2061–2069. [CrossRef]
238. Skarmoutsos, G.A.; Gyftakis, K.N.; Mueller, M. Analytical Prediction of the MCSA Signatures under Dynamic Eccentricity in PM Machines with Concentrated Non-Overlapping Windings. *IEEE Trans. Energy Convers.* **2022**, *37*, 1011–1019. [CrossRef]
239. Zhan, H.; Wu, L.; Lyu, Z.; Du, Y.; Duan, R. Detecting Eccentricity Fault in Permanent Magnet Synchronous Machines by Means of Zero-Sequence Voltage Component. *IEEE Trans. Ind. Appl.* **2024**, *60*, 6761–6774. [CrossRef]
240. Zhou, S.; Ma, C.; Zhu, C.; Wang, J.; Gao, Y.; Wei, Y.; Liu, Z.; Feng, Q. A New Dynamic Eccentricity Diagnosis Method for Permanent Magnet Motors Considering Variable-Speed and Speed Fluctuation Conditions. *IEEE Trans. Instrum. Meas.* **2024**, *72*, 3501012. [CrossRef]
241. Hong, J.; Lee, S.B.; Kral, C.; Haumer, A. Detection of Airgap Eccentricity for Permanent Magnet Synchronous Motors Based on the D-Axis Inductance. *IEEE Trans. Power Electron.* **2012**, *27*, 2605–2612. [CrossRef]
242. Aggarwal, A.; Allafi, I.M.; Strangas, E.G.; Agapiou, J.S. Off-Line Detection of Static Eccentricity of PMSM Robust to Machine Operating Temperature and Rotor Position Misalignment Using Incremental Inductance Approach. *IEEE Trans. Transp. Electrif.* **2021**, *7*, 161–169. [CrossRef]
243. Kang, K.; Song, J.; Kang, C.; Sung, S.; Jang, G. Real-Time Detection of the Dynamic Eccentricity in Permanent-Magnet Synchronous Motors by Monitoring Speed and Back EMF Induced in an Additional Winding. *IEEE Trans. Ind. Electron.* **2017**, *64*, 7191–7200. [CrossRef]
244. Wang, Y.; Liu, K.; Hua, W.; Zhang, C.; Wu, Z.; Zhang, H. Analysis and Detection of Rotor Eccentricity in Permanent Magnet Synchronous Machines Based on Linear Hall Sensors. *IEEE Trans. Power Electron.* **2022**, *37*, 4719–4729. [CrossRef]
245. Ehya, H.; Nysveen, A.; Antonino-Daviu, J.A. Advanced Fault Detection of Synchronous Generators Using Stray Magnetic Field. *IEEE Trans. Ind. Electron.* **2022**, *69*, 11675–11685. [CrossRef]
246. Ehya, H.; Nysveen, A.; Nilssen, R.; Liu, Y. Static and Dynamic Eccentricity Fault Diagnosis of Large Salient Pole Synchronous Generators by Means of External Magnetic Field. *IET Electr. Power Appl.* **2021**, *15*, 890–902. [CrossRef]
247. Cui, H.; Ma, C.; Wang, Y.; Li, X.; He, Y.; Shen, Z.; Ji, Z.; Wang, P. Analytical Calculation of Stray Magnetic Field in Interior Permanent Magnet Synchronous Motor Under Static Eccentricity Considering Nonlinear and Non-Uniform Magnetic Saturation. *IEEE Trans. Magn.* **2024**, *61*, 8200411. [CrossRef]
248. He, Y.-L.; Zhang, Z.-J.; Tao, W.-Q.; Wang, X.-L.; Gerada, D.; Gerada, C.; Gao, P. A New External Search Coil Based Method to Detect Detailed Static Air-Gap Eccentricity Position in Nonsalient Pole Synchronous Generators. *IEEE Trans. Ind. Electron.* **2021**, *68*, 7535–7544. [CrossRef]
249. Park, J.-C.; Park, S.-H.; Kim, J.-H.; Lee, S.-G.; Lee, G.-H.; Lim, M.-S. Diagnosis and Robust Design Optimization of SPMSM Considering Back EMF and Cogging Torque Due to Static Eccentricity. *Energies* **2021**, *14*, 2900. [CrossRef]
250. Hsieh, M.-F.; Yeh, Y.-H. Rotor Eccentricity Effect on Cogging Torque of PM Generators for Small Wind Turbines. *IEEE Trans. Magn.* **2013**, *49*, 1897–1900. [CrossRef]
251. Chen, Z.; Wang, F.; Fan, C.; Ling, Z.; Li, Z.; Wang, Q. Analysis of Rotor Eccentricity Fault in IPMSM With Different Armature Winding Structures. *IEEE Trans. Magn.* **2023**, *59*, 8100410. [CrossRef]
252. Du, J.; Zhong, R.; Wu, Z.; Hua, W.; Wu, Z.; Zhang, C. Effect of Eccentricity on Vibration and Noise of External-Rotor PMSM. In Proceedings of the 2024 International Conference on Electrical Machines (ICEM), Torino, Italy, 1–4 September 2024; IEEE: Piscataway, NJ, USA, 2024; pp. 1–6.
253. Ma, C.; Zuo, S. Black-Box Method of Identification and Diagnosis of Abnormal Noise Sources of Permanent Magnet Synchronous Machines for Electric Vehicles. *IEEE Trans. Ind. Electron.* **2014**, *61*, 5538–5549. [CrossRef]
254. Kang, J.-K.; Hur, J. Static Eccentric Fault Diagnosis of IPMSM Using Thermocouple Sensor. In Proceedings of the 2023 IEEE Energy Conversion Congress and Exposition (ECCE), Nashville, TN, USA, 29 October–2 November 2023; IEEE: Piscataway, NJ, USA, 2023; pp. 4465–4468.
255. Ebrahimi, B.M.; Faiz, J.; Araabi, B.N. Pattern Identification for Eccentricity Fault Diagnosis in Permanent Magnet Synchronous Motors Using Stator Current Monitoring. *IET Electr. Power Appl.* **2010**, *4*, 418–430. [CrossRef]
256. Ebrahimi, B.M.; Javan Roshtkhari, M.; Faiz, J.; Khatami, S.V. Advanced Eccentricity Fault Recognition in Permanent Magnet Synchronous Motors Using Stator Current Signature Analysis. *IEEE Trans. Ind. Electron.* **2014**, *61*, 2041–2052. [CrossRef]
257. Sun, W.; Wang, H.; Qu, R. A Novel Data Generation and Quantitative Characterization Method of Motor Static Eccentricity with Adversarial Network. *IEEE Trans. Power Electron.* **2023**, *38*, 8027–8032. [CrossRef]

258. Wang, H.; Sun, W.; Jiang, D.; Liu, Z.; Qu, R. Rotor Eccentricity Quantitative Characterization Based on Physics-Informed Adversarial Network and Health Condition Data Only. *IEEE Trans. Ind. Electron.* **2024**, *71*, 6738–6752. [CrossRef]
259. Song, J.; Wu, X.; Qian, L.; Lv, W.; Wang, X.; Lu, S. PMSLM Eccentricity Fault Diagnosis Based on Deep Feature Fusion of Stray Magnetic Field Signals. *IEEE Trans. Instrum. Meas.* **2024**, *73*, 3506012. [CrossRef]